Understanding the development of human bladder cancer by using a whole-organ genomic mapping strategy

Tadeusz Majewski[1,*], Sangkyou Lee[1,*], Joon Jeong[1], Dong-Sup Yoon[1], Andrzej Kram[1], Mi-Sook Kim[1], Tomasz Tuziak[1], Jolanta Bondaruk[1], Sooyong Lee[1], Weon-Seo Park[1], Kuang S Tang[2], Woonbok Chung[3], Lanlan Shen[3], Saira S Ahmed[3], Dennis A Johnston[2], H Barton Grossman[4], Colin P Dinney[4], Jain-Hua Zhou[5], R Alan Harris[6], Carrie Snyder[7], Slawomir Filipek[8], Steven A Narod[9], Patrice Watson[7], Henry T Lynch[7], Adi Gazdar[10], Menashe Bar-Eli[11], Xifeng F Wu[12], David J McConkey[4], Keith Baggerly[2], Jean-Pierre Issa[3], William F Benedict[5], Steven E Scherer[6] and Bogdan Czerniak[1]

The search for the genomic sequences involved in human cancers can be greatly facilitated by maps of genomic imbalances identifying the involved chromosomal regions, particularly those that participate in the development of occult preneoplastic conditions that progress to clinically aggressive invasive cancer. The integration of such regions with human genome sequence variation may provide valuable clues about their overall structure and gene content. By extension, such knowledge may help us understand the underlying genetic components involved in the initiation and progression of these cancers. We describe the development of a genome-wide map of human bladder cancer that tracks its progression from *in situ* precursor conditions to invasive disease. Testing for allelic losses using a genome-wide panel of 787 microsatellite markers was performed on multiple DNA samples, extracted from the entire mucosal surface of the bladder and corresponding to normal urothelium, *in situ* preneoplastic lesions, and invasive carcinoma. Using this approach, we matched the clonal allelic losses in distinct chromosomal regions to specific phases of bladder neoplasia and produced a detailed genetic map of bladder cancer development. These analyses revealed three major waves of genetic changes associated with growth advantages of successive clones and reflecting a stepwise conversion of normal urothelial cells into cancer cells. The genetic changes map to six regions at 3q22–q24, 5q22–q31, 9q21–q22, 10q26, 13q14, and 17p13, which may represent critical hits driving the development of bladder cancer. Finally, we performed high-resolution mapping using single nucleotide polymorphism markers within one region on chromosome 13q14, containing the model tumor suppressor gene *RB1*, and defined a minimal deleted region associated with clonal expansion of *in situ* neoplasia. These analyses provided new insights on the involvement of several non-coding sequences mapping to the region and identified novel target genes, termed forerunner (FR) genes, involved in early phases of cancer development.
Laboratory Investigation (2008) **88,** 694–721; doi:10.1038/labinvest.2008.27; published online 5 May 2008

KEYWORDS: forerunner genes; whole-organ histologic and genetic mapping; high-resolution mapping with SNPs; dual-track pathway of bladder cancer development; apoptosis

We have developed a strategy to identify genetic hits across the entire mucosa of an affected organ relative to cancer progression, from *in situ* precursor conditions to invasive disease, on a total genomic scale. We used the approach, which we refer to as whole-organ histologic and genetic mapping (WOHGM), to identify clonal hits associated with growth advantage, thus tracking the development of human bladder cancer from occult *in situ* lesions. Human bladder carcinoma was used as a model of a common epithelial malignancy that develops by progression of microscopically recognizable intraurothelial preneoplastic conditions known as dysplasia and carcinoma *in situ*.[1]

Carcinoma of the bladder is the fifth most frequent human cancer, primarily affecting people over the age of 50 years, and accounts for approximately 3% of all cancer-related deaths.[2,3] The common carcinomas of the bladder develop in its epithelial lining (urothelium) and are referred to as transitional cell carcinomas (TCCs). They arise via two distinct, but sometimes overlapping pathways, papillary and non-papillary.[4,5] Approximately 80% of urinary bladder tumors are superficially growing papillary lesions that originate from urothelial hyperplasia. They frequently recur after excision but usually do not aggressively invade the bladder wall or metastasize. Most aggressive bladder cancers are of the solid, non-papillary type, which originate from *in situ* precursor conditions such as dysplasia and carcinoma *in situ*. They aggressively invade the bladder wall and have a high propensity for metastasis. Exposure to environmental, industrial, and habitual chemical carcinogens has a well-established etiologic relation to bladder cancer.[6] Cigarette smoking is the most important risk factor, thought to contribute to more than 50% of cases, while occupational or environmental exposure to aromatic amines may account for an additional 25% of the total.[7,8]

The maps of several individual chromosomes and the preliminary genetic model of bladder carcinogenesis based on deletional maps of chromosomes 4, 8, 9, 11, and 17 constructed by WOHGM were reported previously.[9–15] The genome-wide WOHGM data were included in our recent publication focused on the concept of alternative target genes termed forerunner (FR) genes located near the model tumor suppressor, *RB1*.[16]

Here, we report on the construction of the genome-wide map that tracks human bladder cancer development from *in situ* precursor conditions to clinically aggressive invasive disease. We present the principles of WOHGM and describe the integration of deletional recombination-based chromosomal maps with the human genome sequence maps using chromosome 13 as an example. This approach was extended to the remaining autosomes and permitted the construction of a genome-wide map of bladder cancer as well as the identification of the six chromosomal regions critical for its development.

Finally, we present high-resolution mapping with single nucleotide polymorphism (SNP) markers of one of the critical chromosomal regions that contains the model tumor suppressor, *RB1* on chromosome 13q14, which defined a minimal deleted segment associated with clonal expansion of *in situ* neoplasia. The analysis of its genomic content provided insight into the role of both non-coding sequence and FR genes involved in early phases of bladder carcinogenesis.

MATERIALS AND METHODS
Overall Strategy
The overall strategy used to construct a genome-wide map of bladder cancer development is summarized in Figure 1. For WOHGM the initial primary screening with hypervariable DNA markers was performed on paired non-tumor (peripheral blood) and representative invasive tumor DNA samples of five cystectomy specimens. Markers showing loss of heterozygosity (LOH) were selected for secondary screening on all mucosal samples of the same cystectomy specimens. The pattern of LOH of chromosomes 1–22 was used to construct a genome-wide map of bladder cancer development and to identify six chromosomal regions critical for clonal expansion of *in situ* neoplasia. Since these six regions were identified by testing five cystectomy specimens, we validated the frequency of their involvement on paired voided urine and peripheral blood DNA (PBDNA) samples from 63 bladder cancer patients.

We concentrated our subsequent high-resolution WOHGM studies on one of the critical chromosomal regions spanning 26.9 Mb around a model tumor suppressor *RB1*. These studies defined a 1.34 Mb minimal deleted region flanking *RB1*, which contained several positional alternative target FR genes putatively involved in clonal expansion of *in situ* neoplasia. The WOHGM studies were verified on 111 paired bladder tumors and PBDNA. The organization of high-resolution mapping studies followed by the analysis of genomic content of the 13q14 minimal deleted region and its candidate FR genes is shown in Figure 2.

Human samples and cell lines
Bladder tumor samples used in our study were classified according to the three-tier histologic tumor grading system of the World Health Organization[17] and were dichotomized into low-grade (grade 1–2) and high-grade (grade 3) tumors.[5] The growth pattern of papillary *versus* non-papillary or solid and the depth of invasion were also recorded. Levels of invasion were defined according to the TNM staging system.[18] T_1 tumors were substaged into superficial (T_a–T_{1a}) and invasive (T_{1b} and higher) groups.[19,20] The precursor intraurothelial lesions were dichotomized into low- and high-grade categories labeled LGIN and HGIN, respectively, as previously described.[5] All human tissues were collected under protocols reviewed and approved by the Institutional Review Boards of the participating institutions and their sharing was carried out under the inter-institutional material transfer agreements.
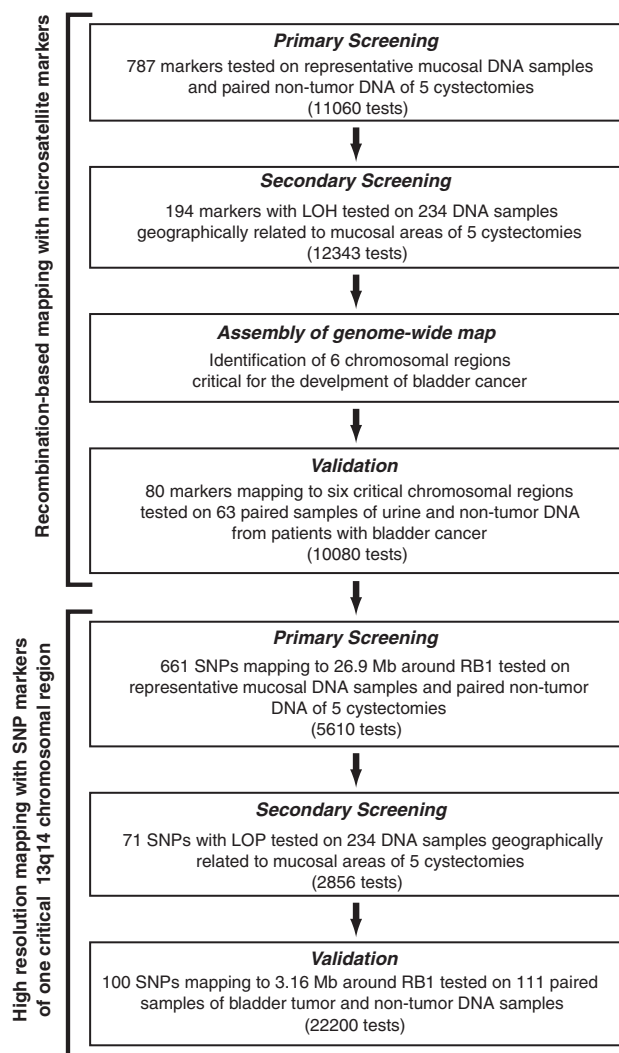
Figure 1 Strategy used to construct genomic model of bladder cancer. The primary screening with hypervariable DNA markers was performed on paired samples of non-tumor and invasive tumor DNA. Markers showing LOH were selected for secondary screening on all mucosal samples of the same cystectomy. Markers mapping to autosomes 1–22 were tested on five cystectomy specimens. The pattern of LOH on chromosomes 1–22 was used to construct a genome-wide map of bladder cancer development and to identify six chromosomal regions critical for clonal expansion of *in situ* neoplasia. Finally, the high-resolution mapping was performed on one of the critical chromosomal regions containing a model tumor suppressor, *RB1*. These studies defined a minimal deleted region associated with clonal expansion of intraurothelial neoplasia around *RB1* and permitted the identification of novel target FR genes providing growth advantage for this expansion.

WOHGM was performed on radical cystectomy specimens from five patients with previously untreated sporadic high-grade (grade 3) invasive TCC. All patients were men, ranging in age from 47 to 78 years (mean = 66.4 ± 11.9 years s.d.). The genome-wide WOHGM with hypervariable DNA markers was used to identify six chromosomal regions critical for clonal expansion of *in situ* neoplasia. The frequency of their involvement was verified on paired voided urine and PBDNA

samples from 63 bladder cancer patients. The 63 patients were comprised of 46 men and 17 women, with ages ranging from 45 to 86 years (mean age = 68.5 ± 10.6 years s.d.). Among 63 TCCs, 28 were low-grade (grade 1–2) superficial (T_a–T_{1a}) and 35 were high-grade (grade 3) invasive (T_{1b} and higher) tumors. For 32 of these patients, the voided urine was collected at the time of initial diagnosis. The remaining 31 patients had a history of bladder tumor removal by transurethral resection and were disease free at the time of urine collection.

The high-resolution WOHGM with SNP markers was performed on the *RB1*-containing 13q14 region using the same five cystectomy specimens. The high-resolution WOHGM studies were verified on an additional 111 paired samples of bladder tumors and PBDNA. The 111 patients were comprised of 86 men and 25 women (mean age 66.1 ± 10.5 years s.d.). Among 111 TCCs, 20 were low-grade (grade 1–2) superficial (T_a–T_{1a}) and 91 were high-grade (grade 3) invasive (T_{1b} and higher) tumors.

We analyzed the sequences, expression, and methylation status of the candidate FR genes using cystectomy specimens, bladder cancer cell lines, and paired samples of adjacent urothelium and bladder tumors. In the first instance, the human bladder cancer cell lines UC1, UC2, UC3, UC6, UC9, UC10, UC12, UC13, UC15, UC16, and UC17, and normal human urothelial cells were established by us and the SV40 immortalized human urothelial cell line, SVHUC was obtained from Dr CA Reznikoff; cells were cultured as previously described.[21–25] In the second instance, the same five cystectomy specimens utilized for genome-wide mapping studies were used for geographic sequencing of selected candidate FR genes. In the third instance, the expression and methylation studies were conducted on paired samples of adjacent urothelium and tumor from patients with bladder cancer. In addition, large-scale testing for methylation of *ITM2B* and sequencing of *P2RY5* were performed on multiple bladder tumor samples as previously described.[16] Because in some instances point mutations of *P2RY5* affected the germ line, and our patients or their family members were not able to provide meaningful familial histories, we performed additional sequencing analyses of index cases from 46 families with high incidences of various common malignancies. The clinical data with a list of tumors affecting these families are provided in Supplementary Table 1.

To verify that loss of FR gene function is a frequent phenomenon in human carcinogenesis, the sequence, methylation status, and expression of *RB1* and selected candidate FR genes were tested in 62 cell lines derived from several groups of human malignancies. We established cell lines or obtained them from the American Type Culture Collection (Manassa, VA, USA) and cultured them as previously described.[26,27]

WOHGM with hypervariable DNA markers
A genome-wide search for chromosomal regions, whose losses are associated with growth advantage and clonal
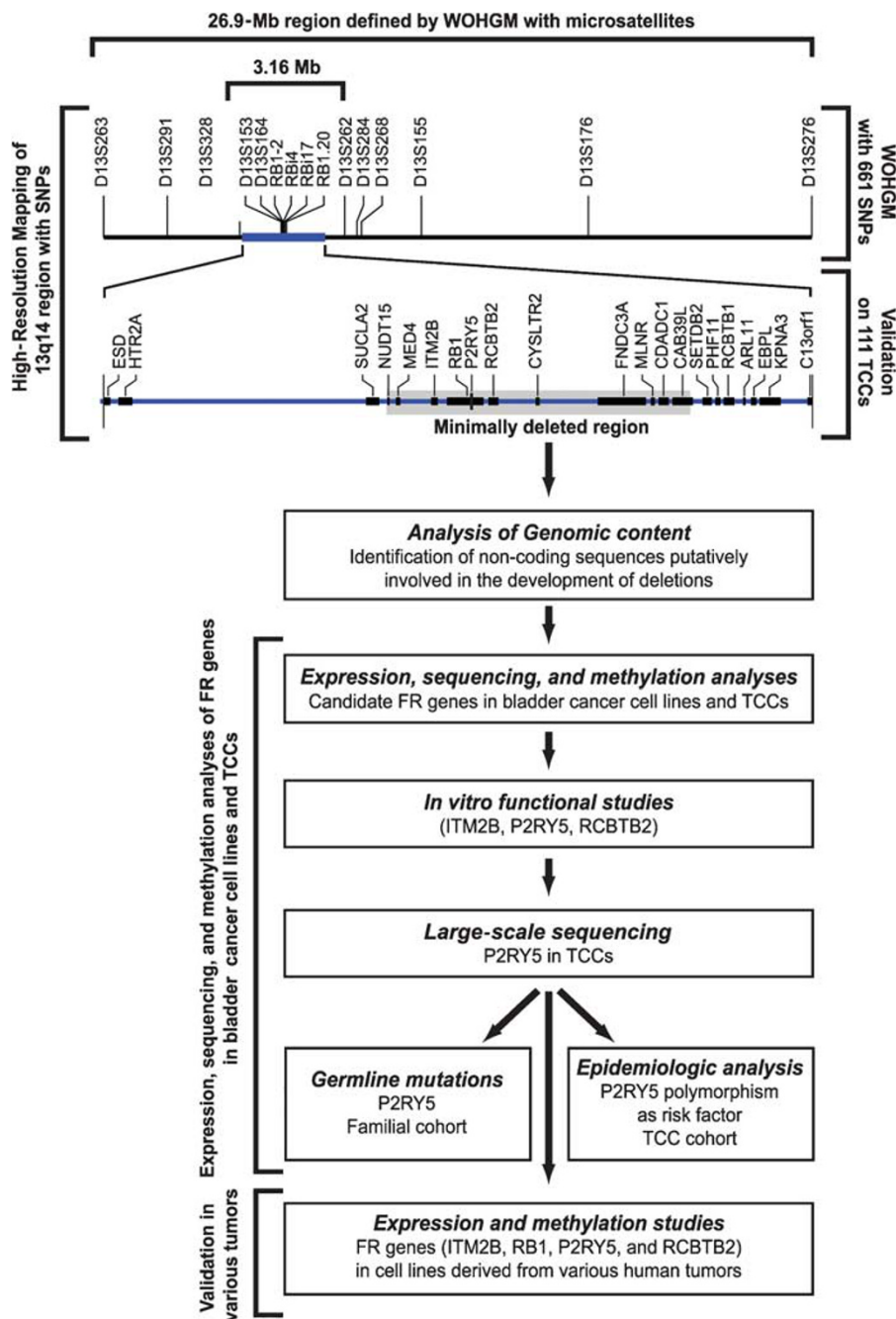
Figure 2 Organization of the high-resolution mapping studies of 13q14 region. The high-resolution mapping studies of 26.9 Mb in the 13q14 region containing *RB1* were performed with SNP markers using WOHGM strategy. The frequency of involvement of a 1.34-Mb minimal deleted region around *RB1* was confirmed on 111 samples of bladder tumors by allelotyping of 100 SNPs mapping across 3.16-Mb segment around *RB1*. The mapping studies were followed by the genomic content analysis of the minimal deleted region, as well as expression, sequencing, methylation, and *in vitro* functional studies of its positional candidate FR genes. Some of the studies outlined here were previously published[16] and are complemented with the new analyses included in this paper.

expansion of *in situ* neoplasia, was performed by WOHGM using hypervariable DNA markers and human cystectomy specimens as previously described.[9–15] In brief, each fresh cystectomy specimen was opened longitudinally along the anterior wall of the bladder and pinned down to a paraffin block. The entire bladder was divided into 1 cm × 2 cm rectangular samples and frozen in OCT. Several 5-µm thick sections were cut from each frozen block. One frozen section from each block was stained with hematoxylin and eosin to evaluate the distribution of *in situ* precursor lesions and TCC microscopically. The remaining unstained sections were stored at −70°C until used for immunohistochemical studies.

Figure 3 Maps of cystectomy specimens used for whole-organ genomic mapping. The distribution of *in situ* precursor lesions and TCC is shown in each individual cystectomy according to the histologic map code. Foci of carcinoma are outlined by a continuous red line. The histologic grade, pathogenetic subset, and stage for each focus of carcinoma are provided. The histologic map code is as follows: 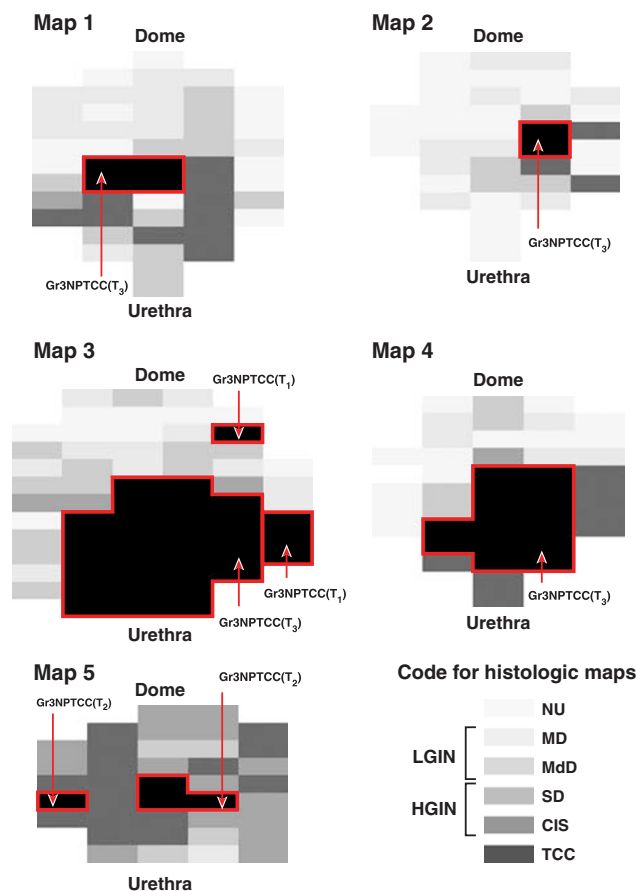NU, normal urothelium; MD, mild dysplasia; MdD, moderate dysplasia; SD, severe dysplasia; CIS, carcinoma *in situ*; TCC, transitional cell carcinoma; LGIN, low-grade intraurothelial neoplasia; and HGIN, high-grade intraurothelial neoplasia.

The whole-organ maps of cystectomy specimens with the distribution of *in situ* precursor lesions and TCC are shown in Figure 3. For DNA extraction, the mucosal samples were defrosted and washed three times in PBS. The mucosal surface of each sample containing microscopically normal-appearing urothelium or *in situ* precursor lesions (LGIN and HGIN) was scraped with a razor blade and transferred into a conical tube containing PBS. In samples with invasive TCC, the tumor tissue was dissected from the frozen block to minimize contamination with non-tumor cells. Only those samples that yielded more than 90% microscopically recognizable intact urothelial tumor cells were used for DNA extraction. This procedure provided 49, 39, 65, 42, and 39 DNA samples, respectively, from the five cystectomies. As a control, DNA extracted from the peripheral blood lymphocytes and/or from normal tissue in the resected specimen of each patient was used.

WOHGM was performed with a set of primers for 787 DNA markers (mostly microsatellites) mapping to chromosomes 1–22 and based on the integrated sex-averaged microsatellite map from Genethon (version March 1996) and updated by the Cooperative Human Linkage Center (version 4.0) (Research Genetics, Huntsville, AL, USA). Markers mapping to chromosomes X and Y were not tested. Testing with DNA hypervariable markers was performed in two steps. In the first step, all 787 markers were tested on paired samples corresponding to non-tumor and invasive tumor DNA from the same individual in five cystectomy specimens. Those markers that showed allelic loss were tested on all mucosal samples of the same cystectomy. The allelic patterns of markers were resolved on 6% polyacrylamide gels after their amplification using the PCR. An additional set of 80 microsatellite DNA markers mapping to the six chromosomal regions associated with clonal expansion of neoplasia was tested on DNA extracted from voided urine sediments from 63 patients with bladder cancer. The raw data used to assemble the genomic map of bladder cancer development are summarized in Table 1.

Analysis of Human Genome Sequence Databases Spanning the Deleted Regions
During generation of these data, resources defining the human genome evolved from integrated genetic and radiation hybrid maps to physical maps, to the draft sequence and finally to the finished human genome sequence. We primarily used the Santa Cruz browser (http://genome.ucsc.edu) and secondarily, the browsers and maps available from Ensembl (http://www.ensembl.org) and the NCBI Integrated Map Viewer (http://www.ncbi.nlm.nih.gov/mapview/map_search.cgi?taxid = 9606) to place the hypervariable markers on the genomic sequence using their available tracks. We also used these resources to extract the relevant known and predicted genes, EST clusters, SNPs, and CpG islands corresponding to these regions of interest. Finally, for markers not present on tracks, we used electronic PCR, *in silico* PCR, or BLAST for placement.[28–30]

Statistical Analysis
The data were organized and analyzed as previously described.[14] In brief, the information on LOH of individual markers was entered into a database and superimposed over the histologic maps. Initial data consisted of chromosomal vectors with a list of markers with their LOH and coordinates for locations of mucosal samples, which could be used to plot the distribution of LOH to microscopically classified urothelial changes. By superimposing plots of LOH over the histologic maps, we identified the areas of bladder mucosa with altered markers and analyzed their relationship to intraurothelial precursor conditions and invasive cancer.

The relationship between altered markers and the progression of urothelial neoplasia from precursor conditions to invasive cancer was initially tested by a binomial maximum

Table 1 Summary of data used for assembly of genome-wide map of bladder cancer

Chromosomes	Average distance between markers (cM)	Number of markers	First screening (no. of tests)	Secondary screening (no. of tests)
1	6.86	54	756	819
2	8.26	45	630	925
3	6.70	36	504	289
4	4.77	45	630	900
5	7.83	33	546	1010
6	5.40	42	546	650
7	5.32	43	602	84
8	3.75	43	602	565
9	3.24	52	728	1012
10	5.11	35	490	780
11	3.19	47	658	1163
12	4.91	38	532	73
13	3.03	42	588	789
14	4.80	31	434	163
15	4.89	30	420	98
16	4.52	30	420	646
17	3.79	38	532	1152
18	4.61	29	406	611
19	4.54	23	322	123
20	5.43	21	294	30
21	4.31	16	224	234
22	5.25	14	196	227
	Average 5.03	Totals: 787	11 060	12 343

likelihood analysis, and the significance of the relationship was expressed as a logarithm of odds (LOD) score as previously described.[10–13,16,31] We chose LOD scores because they represent a powerful method of likelihood analysis that can verify the statistical significance of the relationship among patterns of sequential events. The LOD scores were applied in their generic mathematical sense as likelihood tests of events. In sporadic cancer when microscopically defined stages of cancer progression are used as standards of sequential events and there is mitotic transmission of the phenotype, the null hypothesis is more appropriately verified at a recombination factor differing from 0.5. Hence, combined LOD scores for all cystectomies were calculated at variable $\theta = 0.01$, 0.5, and 0.99. A pattern of LOD scores $\geqslant 3$ at $\theta = 0.01$ or 0.99 and LOD scores < 3 at $\theta = 0.5$ for the same marker was considered significant. The strongest association between altered marker and neoplasia was when a

LOD score was $\geqslant 3$ and $\theta = 0.99$ and 0.5 and < 3 at $\theta = 0.01$. Stringency 1 designated LOD scores for specific stages of neoplasia. Stringency 2 designated LOD scores for progression to higher stages of neoplasia. The relationships among LOH in individual loci and various clinico-pathological parameters of tumors and voided urine samples were tested by Gehan's generalized Wilcoxon and log-rank tests ($P \leqslant 0.05$ was considered significant).

The genome-wide patterns of LOH in relation to geographic distribution of preneoplastic conditions and invasive cancer in individual cystectomies were generated and analyzed by the nearest neighbor algorithm.[32]

High-resolution mapping with SNPs of the 13q14 region containing RB1

WOHGM with SNPs was performed as previously described.[14] In brief, the genome sequence corresponding to the microsatellite-defined region of LOH in 13q14 was assembled. The positions of all currently defined SNPs mapping within the 26.9-Mb region around *RB1* (approximately 20 000 SNPs) were identified in the SNP database (http://www.ncbi.nlm.nih.gov/SNP). The integrated gene and SNP map was used to select 661 SNPs mapping within a 26.9-Mb segment around *RB1*. Allelotyping of SNPs was performed and analyzed using an automated pyrosequencing instrument PSQ96MA (Biotage AB, Uppsala, Sweden).[33,34] The SNPs were sequenced using DNA samples corresponding to whole-organ histologic maps of five cystectomy specimens originally used for microsatellite-based WOHGM. The minimal deleted region associated with clonal expansion of *in situ* neoplasia was identified by the alignment of clonal plaque-like deleted segments from individual cystectomies. Additional allelotyping of 100 SNPs mapping between the *ESD* and *C13orf1* genes and spanning approximately 3.16 Mb around *RB1* was performed using SNP multiplex (SNPlex™; Applied Biosystems, Foster City, CA, USA) technology following the manufacturer's protocol available at http://docs.appliedbiosystems.com/pebiodocs/04360857.pdf.

Immunohistochemical staining for RB protein

RB protein status was determined by immunohistochemical analysis of frozen sections using the RB-WL-1 polyclonal anti-RB antibody as previously described.[35,36] In brief, RB-WL-1 is a rabbit polyclonal antibody produced against a peptide encoded by exon 10 of *RB1*. In western blot analyses, to recognize both phosphorylated and underphosphorylated forms of the RB protein, staining could be completely blocked by an excess of the immunizing peptide. For immunohistochemical staining, frozen sections stored at $-70°$C were defrosted for 30 min at room temperature and fixed in cold methanol: acetone (1:1 volume) at $4°$C for 10 min. After being rinsed three times in PBS, they were incubated for 15 min with 0.1% H_2O_2 in PBS, followed by a 15-min incubation with avidin blocking solution and a 15-min incubation with biotin blocking solution (Vector Laboratories

Inc., Burlingame, CA, USA). The sections were then blocked with 10% goat serum in 2% BSA-PBS for 30 min and incubated overnight at 4°C with RB-WL-1 polyclonal anti-RB antibody at 0.25 μg/ml in 2% BSA-PBS. The bound antibody was visualized by avidin–biotin complex assay using a VECTASTAIN ABC kit (Vector Laboratories Inc.) with 3,3′-diaminobenzidine as the chromogen.

Expression assays for RB1 and candidate FR genes
Quantitative RT-PCR was used to analyze the expression levels of *RB1* and candidate FR genes in cell lines and paired samples corresponding to adjacent urothelium and bladder tumor samples as described previously.[16] For RT-PCR, cDNA was synthesized from 2 μg of total RNA using the TaqMan™ RT reagents following the manufacturer's protocol (Applied Biosystems). The primers and fluorescent probes for each gene were designed using the Assays-by-Design provided by Applied Biosystems. RT-PCR analysis was performed on a Perkin-Elmer/Applied Biosystems 7700 Prism apparatus using 18S RNA as an internal normalization standard. In addition to 18S, the expressions of three housekeeping genes (large ribosomal protein, cyclophylin A, and β-actin) were used to calculate the 90% confidence intervals. The expression levels of each gene were compared to their baseline expression in the corresponding normal tissue. We considered the FR genes to be inactivated when their level of expression was reduced by $\geqslant$75% or $\geqslant$4-fold.

DNA sequence analysis
We sequenced the PCR-amplified exons of *RB1* and candidate FR genes from tumor and control samples by Sanger dideoxy sequencing using Big-Dye Terminator Chemistry. PCR products were purified from unincorporated primers and dNTPs by using exonuclease I and shrimp alkaline phosphatase and subsequent sequencing reactions were analyzed with an ABI 3730 sequencer (Applied Biosystems). Sequence was obtained from both strands and potential mutations were identified using the Mutation Surveyor software (Softgenetics, State College, PA, USA) and confirmed by visual inspection. For selected samples, the presence of mutations was confirmed by sequencing of subcloned amplified exons. Pyrosequencing was used to confirm the loss of a wild-type *P2RY5* allele in bladder mucosa and to confirm the presence of the same mutations among the members of families carrying germline mutations of *P2RY5*. Pyrosequencing after laser micro-dissection (SlmicroCut Molecular Machines and Industries, Knoxville, TN, USA) of paraffin-embedded tumor tissue was also used to document the loss of a wild-type *P2RY5* allele in tumors affecting family members carrying germline mutations of *P2RY5*.[33,34]

Testing for germline mutations of known tumor suppressor genes in families with hereditary cancer
Since 46 families with hereditary cancer used for testing of germline mutations of *P2RY5* were affected primarily by hereditary breast cancer and some showed the pattern of transmission as well as types of cancers suggestive of the involvement of other known cancer predisposing genes, germline mutations involving *BRCA1*, *BRCA2*, *p53*, *PTEN*, *hMLH1*, and *hMSH2*,[37–43] were excluded by testing the PBDNA of the affected index cases. The PBDNA of the same index cases was used for testing for germline mutations of *P2RY5*. The involvement of *BRCA1* and *BRCA2* was excluded in all 46 families by partial sequencing of exons 11 and 13 for *BRCA1* and exons 10 and 11 for *BRCA2*.[37] In addition, both genes were tested for the presence of mutations frequently seen in hereditary breast cancer affecting Ashkenazi Jewish families.[38–45] The involvement of these genes was additionally tested by protein termination assays.[46,47] Some of the families included in the analyses were also tested for germline mutations of *p53*, *PTEN*, *hMLH1*, and *hMSH2* by sequencing.[38,43] In one family with missense germline mutations of *P2RY5* that resulted in amino-acid substitutions, complete sequencing of *p53*, *BRCA1/2*, and of *RB1* of the index cases was performed and disclosed the wild-type sequence for all three genes.

Methylation assays
We used combined bisulfite restriction analysis (COBRA) and methylation-sensitive PCR to identify methylated CpG islands containing the putative promoters of candidate FR genes. The bisulfite treatment of DNA and design of the assay were previously described.[48,49] In brief, bisulfite-modified DNA was amplified by PCR and the amplified products were incubated with restriction enzymes that digest only methylated alleles. The methylation status of CpG sites within the putative promoter regions was confirmed by sequencing of sodium bisulfite-modified DNA. To verify whether expression of FR genes could be restored by promoter demethylation, cell lines showing hypermethylated FR gene promoters were treated with 5-aza-2′-deoxycytidine.

RESULTS AND DISCUSSION
WOHGM
Conventional histologic mapping of invasive, clinically evident cancer and adjacent tissues combined with clinical and epidemiological data gathered during the last 50 years provides compelling evidence that epithelial cancers develop from precursor *in situ* conditions designated as dysplasia or carcinoma *in situ*.[50] These conditions progress to invasive cancer by multiple cumulative molecular events. In fact, the incipient hits occur in normal tissue and many are antecedent to the development of microscopically identifiable precursor lesions. Although genetic models of progression from premalignant conditions have been proposed for several human malignancies, including bladder cancer, the specific events leading to the development and progression of human neoplasia have not been defined.[51–57]

Analysis of genomic imbalances can guide us to those chromosomal regions that contain genes and non-coding

sequences playing a role in tumor development. The functional implications of such imbalances and consequently their pathogenetic significance are largely unknown. Moreover, it is unclear which of the imbalances are primary events relevant to disease progression and which are redundant hits dragged through the progression by mere cosegregation. In familial disorders including cancer predisposing syndromes, a cosegregation of genetic hits with diseased phenotype identifies a predisposing locus and may guide subsequent positional cloning of a target gene.[58,59] Unfortunately, the powerful concepts of genetic linkage analysis in pedigrees cannot be used in the vast majority of human cancers, owing

to their primarily sporadic nature. In cancers that develop from preneoplastic conditions, however, the early events can instead be deduced from the geographic relationship between genomic imbalance and precursor *in situ* conditions (Figure 4a–c).[9–16] The similarity of alterations such as loss of the same allele or the presence of identical molecular alterations in multiple samples corresponding to precursor conditions and invasive cancer disclose their clonal relationship. Taken together, these identify genetic hits that provide growth advantage related to a particular clone of cells collectively referred to as clonal expansion.
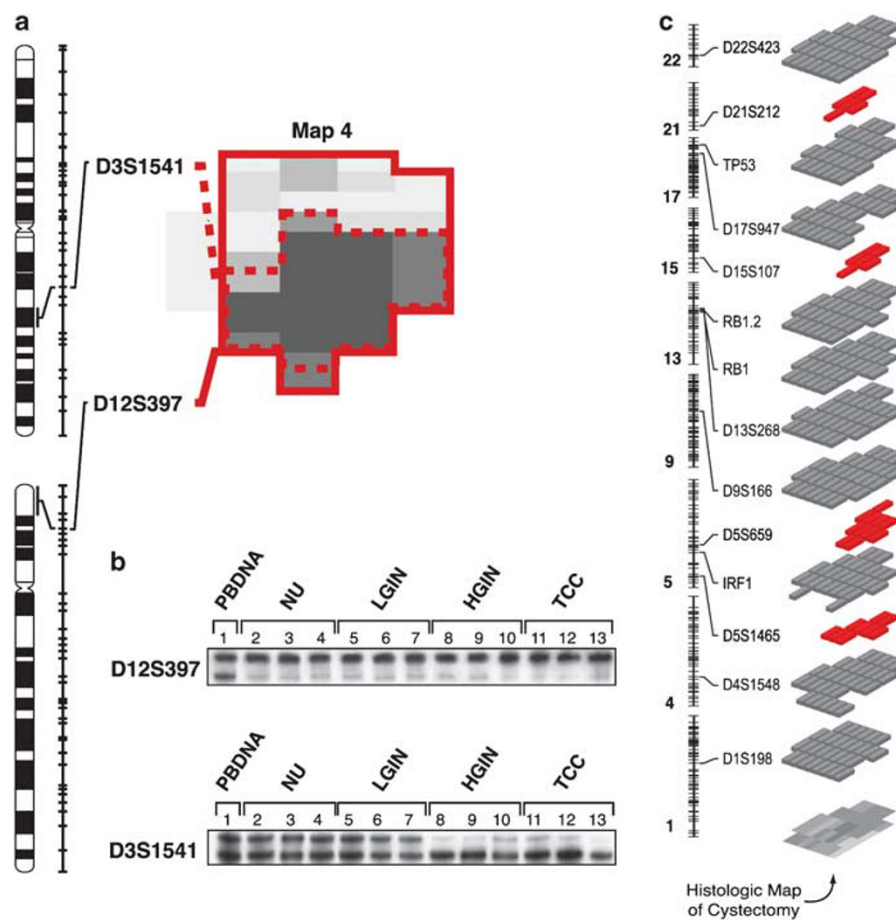

Figure 4 Whole-organ histologic and genetic maps. (**a**) The histologic map of the entire bladder mucosa showing a distribution of intraurothelial neoplastic lesions and invasive cancer is illustrated. For the purpose of statistical analysis, intraurothelial precursor conditions were classified into two groups: low-grade intraurothelial neoplasia (mild to moderate dysplasia, LGIN) and high-grade intraurothelial neoplasia (severe dysplasia and carcinoma *in situ*, HGIN). The areas of bladder mucosa that were involved by clonal allelic losses of markers D3S1541 and D12S397 are delineated by interrupted and continuous red lines, respectively. The positions of these markers on the sex-averaged recombination-based map of chromosomes 3 and 12 as well as their band positions are shown on the left. (**b**) Examples of allelic patterns for the two markers (D12S397 and D3S1541) that were tested on mucosal samples (numbered 1–13) are illustrated. Sample no. 1 shows the allelic pattern of the same marker from peripheral blood lymphocytes (PBDNA) of the same patient. (**c**) Markers exhibiting clonal losses associated with early and late phases of *in situ* bladder neoplasia were identified using a computer algorithm that searched for overlapping plaques that matched the areas of bladder mucosa, with NU and LGIN contiguous to areas of HGIN and TCC (gray blocks). The allelic patterns of markers in mucosal samples were compared to their patterns in peripheral blood lymphocytes of the same patient. The chromosomal regions showing allelic losses restricted to later phases of neoplasia were identified by an algorithm that searched for overlapping plaques of losses restricted to HGIN that had progressed to TCC (red blocks). Markers with non-clonal losses involving smaller independent areas of the mucosa with no geographic relationship to *in situ* neoplasia or invasive cancer were eliminated from the diagram. (Modified and reprinted with permission from Lee S, Jeong J, Majewski T, *et al*. Proc Natl Acad Sci USA 2007;104:13732–13737.)

By superimposing distributions of genetic hits such as allelic loss over the histologic maps of the entire mucosa, the two basic patterns can be identified: scattered, in which several isolated foci are present; and plaque-like, where a large contiguous area of identical genetic changes are found. The scattered isolated foci showing limited clonal expansion of preneoplastic cells are typically not considered to be functionally relevant for disease development and progression (data not shown). The hits that form plaque-like areas associated with clonal *in situ* expansion of preneoplastic cells involving large areas of mucosa that encompass not only invasive cancer and precursor conditions but also adjacent areas of microscopically normal epithelium represent early events associated with the development of incipient occult phases of neoplasia. On the opposite side of the spectrum are hits restricted to invasive carcinoma and adjacent areas of severe dysplasia or carcinoma *in situ*, representing late events associated with the progression to invasive cancer (Figure 4a–c).

For WOHGM, a cystectomy specimen was divided into approximately 30–60 mucosal samples, each covering 2 cm^2 (1 cm × 2 cm) of mucosal area and corresponding to microscopically verified normal urothelium, precursor intraurothelial conditions, or invasive carcinoma. The uroepithelial lining of the bladder was stripped from the underlying stromal tissue by simple mechanical scraping, providing 99% pure urothelial cell suspensions as determined by microscopic evaluation. Such samples typically yielded 5–10 µg of genomic DNA for genome-wide PCR-based mapping studies.

Microsatellite-Based Whole-Organ Histologic and Genetic Map of Chromosome 13

Chromosome 13 was selected as an example because it contains a prototypic tumor suppressor gene, the retinoblastoma (*RB1*) gene.[60,61] The *RB1* locus was originally mapped by chromosomal deletion and genetic linkage in a familial form of retinoblastoma[62–64] and the target *RB1* gene was identified using a positional cloning strategy.[65–68] The inactivation of both *RB1* gene alleles in two distinct steps during the development of retinoblastoma validated the 'two-hit hypothesis'; a key concept of reverse genetics that provided the impetus for the positional cloning of other genes predisposing to various diseases.[69,70] The *RB1* gene was subsequently proven to play a major role in the development of many sporadic human cancers including bladder carcinoma.[71,72] Several studies indicate that the inactivation of *RB1* in bladder neoplasia parallels the onset of severe dysplasia/carcinoma *in situ* that progresses to invasive disease and is associated with an aggressive form of bladder cancer with high propensity for distant metastasis.[73,74] We hypothesized that if our method and approach showed clonal allelic loss of markers mapping to within and around the *RB1* gene, and involving large areas of bladder mucosa, it would be reasonable to assume that similar alterations in other loci

would guide us to novel tumor suppressor-like genes playing a role in early phases of bladder neoplasia.

The initial analysis of paired normal and tumor DNA samples identified LOH in all five cystectomies examined, and involved 14 of 42 tested markers mapping to chromosome 13. The binomial likelihood analysis of LOH distribution patterns across the bladder mucosa showed that allelic losses related to the development of urothelial neoplasia clustered in four distinct regions of chromosome 13. The deleted regions defined by their flanking markers, their predicted size, and a list of markers within regions containing LOH are shown in Figure 5a and b.

A deleted segment mapping to 13q14, flanked by D13S263 and D13S276 and containing the *RB1* gene, showed allelic loss in four of the five cystectomies. Allelic losses in this region were associated with clonal expansion involving large areas of bladder mucosa, encompassing not only invasive cancer and preneoplastic conditions but also extending to areas of microscopically normal urothelium. The allelic losses of markers mapping to within and around the *RB1* gene formed large almost identical overlapping plaques of clonal expansion.

The three remaining segments of allelic losses mapping to 13q12 and 13q13 were associated with some limited clonal expansion and formed several separate foci which were not strictly geographically related to precursor *in situ* lesions.

The entire microsatellite recombination-based deletional maps of chromosomes 1–22 are submitted as Supplementary Figure 1.

Genome-Wide Map of Bladder Cancer Development

The genome-wide search for chromosomal allelic losses using a WOHGM strategy was performed to produce a detailed map of bladder cancer development from occult preneoplastic conditions to invasive disease (Figure 6). We hypothesized that such an approach would also facilitate the analysis of global genetic alterations in multistep bladder carcinogenesis and would permit the identification of the limited number of critical hits that drive the transformation of normal urothelial cells to malignant cells.

The search for losses of genetic material was performed with 787 markers mapping to chromosomes 1–22. Testing was performed on 234 DNA samples from five cystectomies corresponding to microscopically normal urothelium (*n* = 53), LGIN (*n* = 82), HGIN (*n* = 50), and invasive TCC (*n* = 49). Initially all 787 markers were tested on paired DNA samples corresponding to invasive bladder carcinoma and paired normal DNA from peripheral blood lymphocytes. LOH was identified in 194 markers that were subsequently tested on DNA from all mucosal samples from the five cystectomies.

While 72 markers exhibited patterns of LOH that could not be related to the development of progression of bladder neoplasia, the clonal allelic loss of 122 markers clustered in 59 distinct chromosomal regions and had a relationship to the

Figure 5 Deletion map of chromosome 13 assembled from data generated by whole-organ histologic and genetic mapping. (**a**) A list of all tested markers and their positions according to the updated Cooperative Human Linkage Center Map and their chromosomal band locations is shown. Markers printed in red showed statistically significant relationship between LOH and the development of urothelial neoplasia tested by binomial maximum likelihood analyses and calculated as logarithm of odds (LOD) scores. Red bars on the left side of the map identify the deleted regions, which are defined by the positions of deleted markers and their nearest flanking markers with retention of heterozygosity and the predicted size of the deleted regions in centiMorgans. A chromosomal region containing *RB1* flanked by markers D13S263 and D13S276 spanning 26.9 Mb is oriented with genome sequenced map and the positions of all known and predicted genes mapping to this region are shown (cM, centiMorgans; Mb, megabases; WOHGM, whole-organ histologic and genetic mapping of individual cystectomy specimens consecutively numbered 1 through 8. O – markers with retention of heterozygosity, ● – markers with LOH, and Ø – non-informative marker). (**b**) Summary of binomial maximum likelihood analysis testing the relationship among LOH in individual chromosome 13 loci and progression of urothelial neoplasia from *in situ* precursor conditions to invasive TCC. The allelic patterns of markers in mucosal samples were compared to their patterns in peripheral blood lymphocytes of the same patient. Cumulative LOD scores for markers with LOH were calculated at variable $\theta = (0.01, 0.5, \text{and } 0.99)$ and tested against T_{max}. The significance of allelic losses in individual loci was analyzed for normal urothelium (NU); low-grade intraurothelial neoplasia (LGIN); high-grade intraurothelial neoplasia (HGIN), and transitional cell carcinoma (TCC). To simplify the data, only stringency 1 calculations are presented. The patterns of significant LOD scores are as described in Materials and methods. Note that significant patterns of LOD scores typically parallel the high T_{max} values (O – LOD score <3; ● – LOD score $\geqslant 3$). Deletional maps of chromosomes 1–22 are provided in Supplementary Figure 1.

geographic distribution of preneoplastic conditions or invasive cancer, as defined by the binomial maximum likelihood analysis. Of these, 83 were associated with expansion of a phenotypically normal clone or early *in situ* preneoplastic conditions consistent with LGIN. The clonal allelic losses of the 26 remaining markers may be related to the development of HGIN or invasive cancer.

When we analyzed the genome-wide distribution of allelic losses in individual cystectomies, it became evident that all areas of bladder mucosa with LOH were geographically related. Even those markers that exhibited allelic loss across several separate areas of mucosa were in fact related and represented successive subclones emerging from a large clonal field change as defined by the nearest neighbor analysis. Thus, losses of genetic material associated with clonal expansion of urothelial cells could be viewed as a succession of hits associated with growth advantage that parallel the gradual change of normal cells to cancer cells.

We identified three major waves of hits that may correspond to the phases of tumorigenesis identified in experimental models and referred to as initiation, promotion, and progression (data not shown). The first wave contributed to clonal expansion of phenotypically normal-appearing urothelial cells that involved large portions of bladder mucosa. The second wave presumably provided additional growth advantage and was associated with clonal expansion of cells showing the first microscopically recognizable features of dysplasia. The third and last wave led to a fully transformed phenotype and was associated with the onset of severe dysplasia/carcinoma *in situ*. Further advancement to invasive cancer was not associated with an additional major loss of genetic material.

The complex pattern of allelic losses identified by WOHGM most likely reflected the overall genomic instability. Many of these alterations were dragged through the progression sequence by mere cosegregation with those hits that were functionally relevant to the development of neoplasia. To identify those critical changes that were most likely driving tumorigenesis, we searched our data for overlapping plaques of clonal allelic losses demonstrating a strict geographic relationship to the two major phases of urothelial neoplasia that are most critical for the development of bladder cancer (Figure 7a and b). The first group consisted of alterations associated with expansion of a dominant clone with no or minimal phenotypic change, which involved large areas of bladder mucosa. The second group consisted of alterations associated with the development of successive clones showing a fully transformed phenotype, ie, those that were related to onset of severe dysplasia/carcinoma *in situ* progressing to invasive cancer. We identified clonal allelic losses with such characteristics in four of the five tested cystectomies, and each one of them showed a unique combination of changes mapping to distinct chromosomal regions (Figure 8a). This indicates that the paths and the sequence of

events that urothelial cells take on their way to malignancy varied widely in individual cancers. When constellations of putative critical losses from four cystectomies were analyzed it became evident that six chromosomal regions, mapping to 3q22–q24, 5q22–q31, 9q21–q22, 10q26, 13q14, and 17p13 and containing well-known target genes with a tumor suppressor function, were involved in more than one case and may represent six critical hits driving the development of human bladder cancer (Figure 8a). This observation was confirmed by the testing of 80 hypervariable DNA markers mapping to the six critical chromosomal regions, on voided urine samples from 63 patients with bladder cancer (Figure 8a and b). LOH affecting at least one of the critical chromosomal regions could be identified in 98% of the samples. The frequency of LOH in each of the chromosomal regions was similar in patients with clinically evident tumor and in patients with history of bladder tumor removed by a transurethral resection (Figure 8c). The frequency of LOH was also similar in low-grade (grade 1–2) superficial (T_a–T_{1a}) and high-grade (grade 3) invasive (T_{1b} and higher) tumors (Figure 8d). Synchronous LOH involving 2–5 critical chromosomal regions was present in approximately 80% of bladder tumors (Figure 8e).

The identification of clonal allelic losses mapping to distinct regions of various chromosomes with almost identical geographic distribution suggests that they were either synchronous, or occurred at a high rate involving closely related successive generations of cells. This in turn implies an unsteady, fluctuating rate of events with waves of genetic hits followed by more stable periods of clonal expansion in tumor development. Our data document that human tumorigenesis is far more complex than it appears from the epidemiologic data,[75,76] and provides evidence that a limited number of critical steps (at least six) are required and can be accompanied by a highly variable constellation of genome-wide hits, which act in concert.

High-Resolution Mapping of *RB1* Region
In this section, we review our previously published data on high-resolution mapping of the 13q14 region, and the concept of alternative target FR genes contiguous to *RB1* involved in clonal expansion of *in situ* neoplasia.[16] We also provide new mapping data and analyses further supporting the concept of FR genes and discuss novel candidate FR genes mapping around *RB1*. In addition, we discuss the non-coding genomic content of the *RB1* flanking region and putative role of its unique non-coding sequences in the development of bladder cancer.

Identification of minimally deleted region flanking RB1
To identify prototypic genes and non-coding sequences that may drive the initial clonal expansion of intraurothelial neoplasia, we concentrated our efforts on the 13q14 region, which contains the model tumor suppressor gene, *RB1*. Initially, the 26.9-Mb deleted region defined by hypervariable
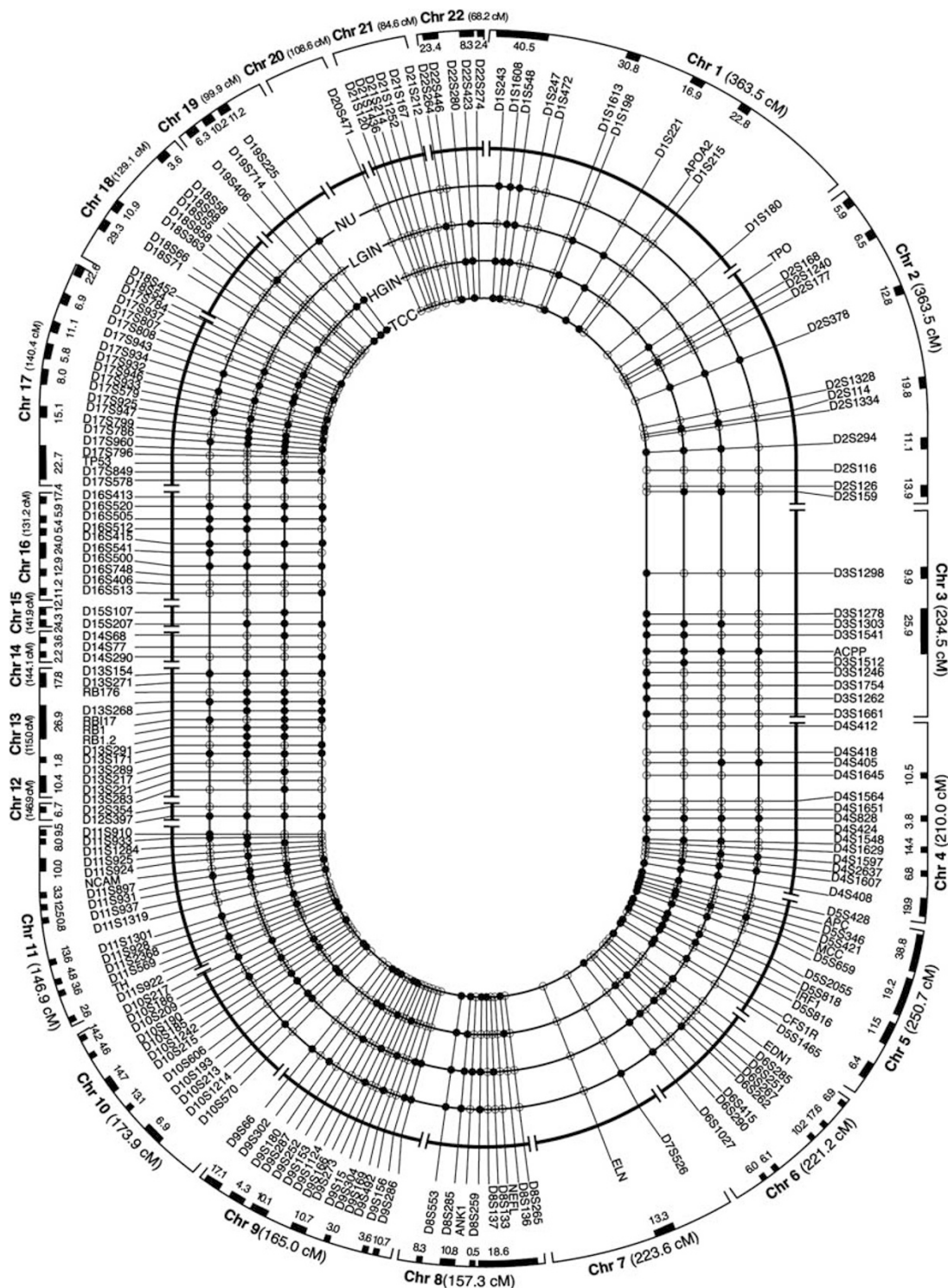
Figure 6 Genome-wide map of bladder cancer progression from intraurothelial precursor conditions to invasive disease. The map was assembled on the basis of whole-organ histologic and genetic mapping of chromosomes 1–22. The outer circle represents chromosomal vectors aligned clockwise from p to q arms with positions of altered markers exhibiting LOH. The innermost concentric circles represent major phases of development and progression of urothelial neoplasia from normal urothelium (NU) through low-grade intraurothelial neoplasia (LGIN), and high-grade intraurothelial neoplasia (HGIN) to transitional cell carcinoma (TCC). The allelic patterns of markers in mucosal samples were compared to their patterns in peripheral blood lymphocytes of the same patient. Solid circles (●) denote statistically significant LOH of the markers defined by the LOD score analysis. Open circles (○) identify LOH without statistically significant association to a given stage of neoplasia. The position of open or solid circles on appropriate concentric circles relates the alterations to a given phase of neoplasia. Only markers with LOH are positioned on the chromosomal vectors. Solid bars on outer brackets represent clusters of markers with significant LOH and denote location of putative chromosomal regions involved in urothelial neoplasia. The distances of markers on chromosomal vectors and the solid bars depicting minimal deleted regions were adjusted to fit the oval and are not drawn to scale.
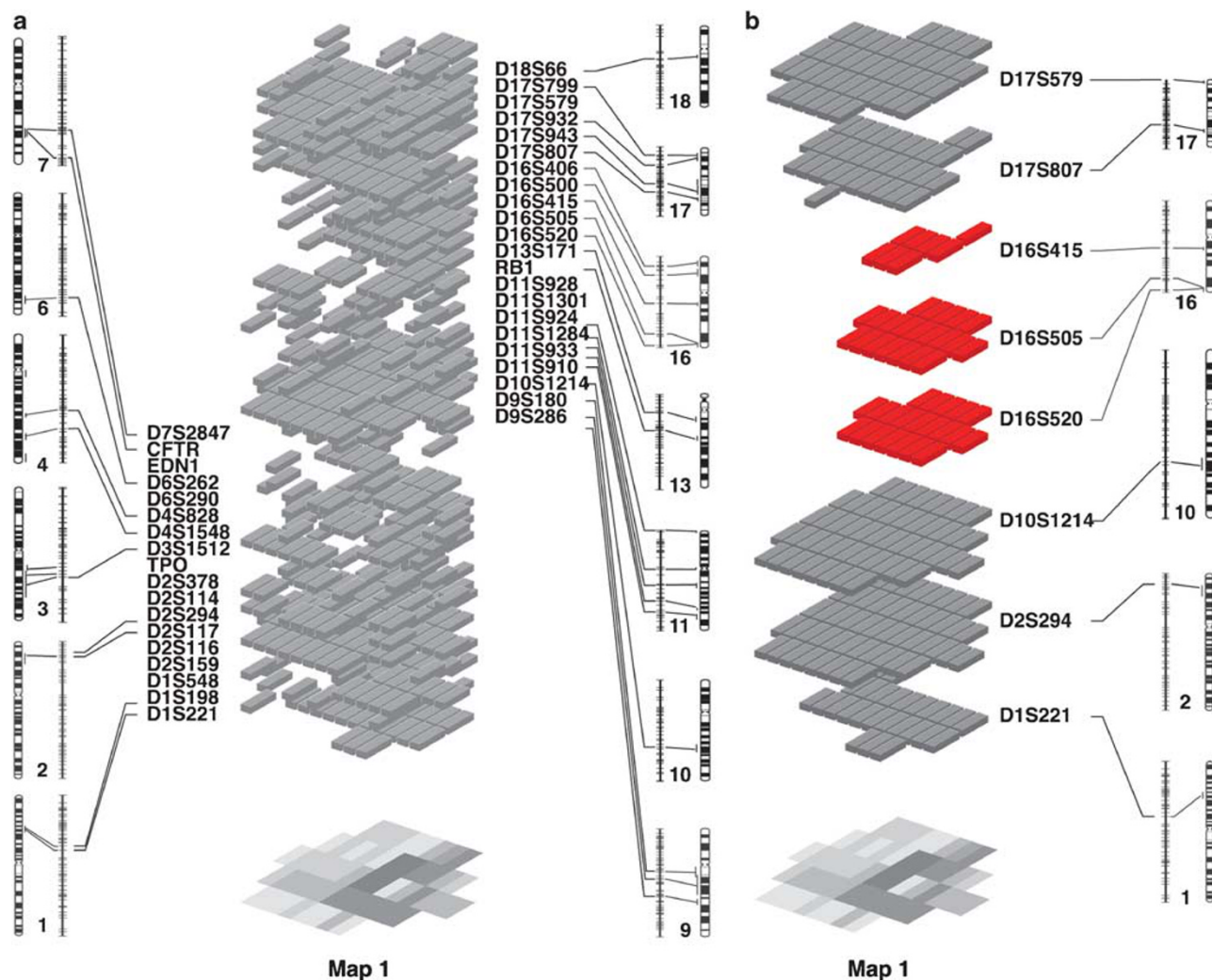
Figure 7 Genome-wide pattern of LOH identified by WOHGM in a single cystectomy. (**a**) Three-dimensional display of the LOH distribution patterns in a single cystectomy specimen. The vertical axis represents sex-averaged recombination-based chromosomal maps with positions of hypervariable markers and their chromosomal location. The shaded blocks represent areas of bladder mucosa with LOH as they relate to the development of bladder cancer from *in situ* neoplasia, represented by a histologic map of the cystectomy shown at the bottom. The allelic patterns of markers in mucosal samples were compared to their patterns in peripheral blood lymphocytes of the same patient. The histologic map code is the same as in Figure 3. (**b**) Clonal losses associated with expansion of *in situ* neoplasia. Chromosomal regions exhibiting allelic losses associated with early and late phases of bladder neoplasia were identified as described in Figure 3.

DNA markers was integrated with the physical map and ultimately with the human genome sequence database. The target region contains over 20 000 SNPs and we selected 661, preferentially located within or around the known and predicted genes, and including 34 SNP mapping within the *RB1* gene. Whole-organ allelotyping of SNPs using the pyrosequencing method was performed in three sequential steps. In the first step, all 661 SNPs of normal genomic DNA from the same individual were sequenced. The number of informative polymorphic SNPs ranged from 76 to 101 in individual cystectomies. In the next step, the polymorphic SNPs were tested on paired normal–invasive tumor samples, and losses of polymorphism (LOP) were identified in all five cystectomies. In the final step, those SNPs that showed LOP

were tested on all mucosal samples. An example of high-resolution mapping with SNPs in one cystectomy specimen is shown in Figure 9a–d. When the whole-organ maps of allelic losses identified by SNPs and hypervariable markers were integrated with *RB1* sequencing data and RB protein expression patterns, it became evident that a loss of DNA that affected *RB1* and flanking regions was an early event in bladder neoplasia (Figure 10a–e). This loss was associated with clonal expansion that formed a plaque involving large areas of bladder mucosa, and was not uniformly associated with the inactivation of the second *RB1* allele (Figure 10b–e). In those cases in which deletion of one *RB1* allele was associated with the inactivation of the second allele by a point mutation accompanied by loss of RB protein expression, the
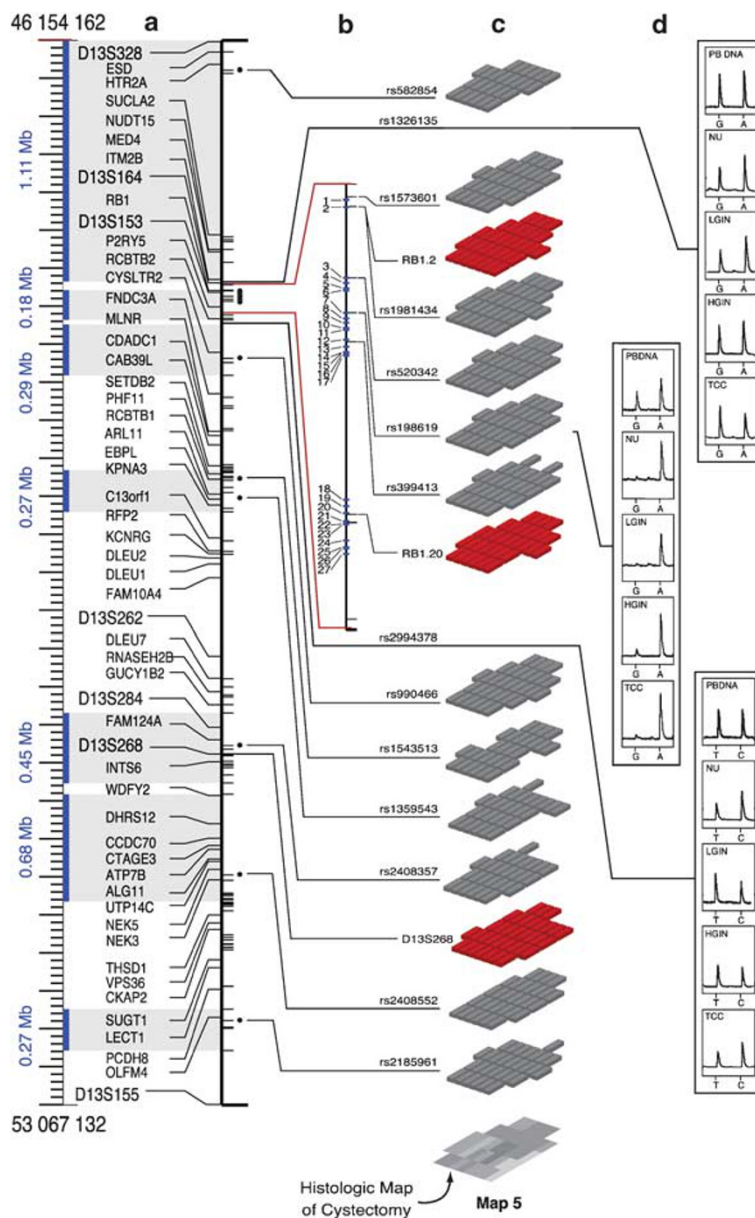
Figure 8 Identification of six critical chromosomal regions involved in the development of bladder cancer. (**a**) Genome-wide map of putative critical hits associated with clonal expansion of intraurothelial neoplasia assembled on the basis of whole-organ histologic and genetic mapping of chromosomes 1–22 as shown in Figure 4. The outer circle depicts a recombination-based map of chromosomes arranged clockwise from p to q arms with positions of markers indicated. The innermost concentric circles represent genetic maps of the four informative cystectomy specimens. Solid green and red dots denote the positions of markers with allelic losses in individual specimens associated with clonal expansion of *in situ* neoplastic lesions progressing to TCC. Green dots designate markers showing LOH associated with early clonal expansion that formed large plaques involving TCC, HGIN, and extended to LGIN or NU. Red dots designate markers with clonal LOH restricted to areas of HGIN and TCC. The recombination-based maps of six critical chromosomal regions are expanded and display the positions of their 80 hypervariable DNA markers. The allelic losses of these markers were tested on DNA extracted from voided urine sediments and paired peripheral blood DNA of 63 patients with bladder cancer. In 32 patients, voided urine was collected at the time of initial diagnosis of primary untreated bladder tumor. The remaining 31 patients had a history of bladder tumor removed by transurethral resection and were disease free at the time of urine collection. (**b**) Frequency of allelic losses identified by individual markers in all 63 DNA samples from voided urine of patients with bladder cancer. (**c**) Frequency of LOH in six critical chromosomal regions in patients with clinically evident tumor and patients with history of bladder cancer and no evidence of disease at the time of testing. (**d**) Frequency of LOH in six critical chromosomal regions in low- (grade 1–2) and high (grade 3)-grade TCCs. (**e**) Frequency of synchronous involvement of one or more critical chromosomal regions identified in voided urine in all 63 patients with bladder cancer. (Modified and reprinted with permission from Lee S, Jeong J, Majewski T, *et al. Proc Natl Acad Sci USA* 2007;104:13732–13737.)

Figure 9 An example of high-resolution whole-organ mapping by allelotyping of SNPs and the assembly of LOH distribution patterns within *RB1*-containing region in a single cystectomy specimen. (**a**) The region containing a cluster of SNPs with allelic loss flanked by markers D13S328 and D13S155 is shown. The bars on the left side indicate the positions of all known and computationally predicted genes. The blue bars on the right side designate the positions of informative polymorphic SNPs. The solid black dots and bars designate SNPs with allelic loss. (**b**) The genomic map of *RB1* is expanded and shows the positions of the five polymorphic SNPs with allelic loss as well as the positions of two polymorphic DNA markers (*RB1.2* and *RB1.20*) with allelic loss. (**c**) The distribution of clonal allelic losses as they relate to precursor *in situ* lesions and invasive TCC shown as a histologic map at the bottom is demonstrated. The blocks depict the distribution of clonal allelic losses identified by the hypervariable DNA markers (red blocks) and SNPs (gray blocks). The allelic patterns of SNP markers in mucosal samples were compared to their patterns in peripheral blood lymphocytes of the same patient. The code for the histologic map is shown in Figure 3. The hypervariable DNA markers and SNPs with allelic loss associated with plaque-like clonal expansion involving large areas of bladder mucosa were clustered within and around *RB1* and involved approximately 7 Mb. These defined several discontinuous regions of allelic losses associated with early clonal expansion of urothelial cells that ranged in size from approximately 0.27–1.11 Mb and are indicated by the vertical blue bars and gray-shaded areas in (**a**). The borders and predicted size of these regions were defined by the nearest flanking SNPs or microsatellite markers that retained polymorphism. The blue numbers indicate the predicted size of the deleted regions. (**d**) An example of clonal loss of a G/A polymorphism in SNP 6 located within intron 12 of *RB1* is illustrated. Non-tumor DNA of peripheral blood lymphocytes of the same patient (PBDNA) shows G/A polymorphism of SNP 6, while samples corresponding to NU, LGIN, HGIN, and TCC show clonal loss of G. Retention of polymorphism in two SNPs flanking a segment of allelic loss that involves the *RB1* gene is also shown. Overall, these data imply that several discontinuous losses of genetic material, which included *RB1* and its flanking regions, occurred in early phases of bladder neoplasia and were associated with *in situ* expansion of a dominant neoplastic clone. (Modified and reprinted with permission from Lee S, Jeong J, Majewski T, *et al*. Proc Natl Acad Sci USA 2007;104:13732–13737; (**c**) and (**d**) represent new data.)
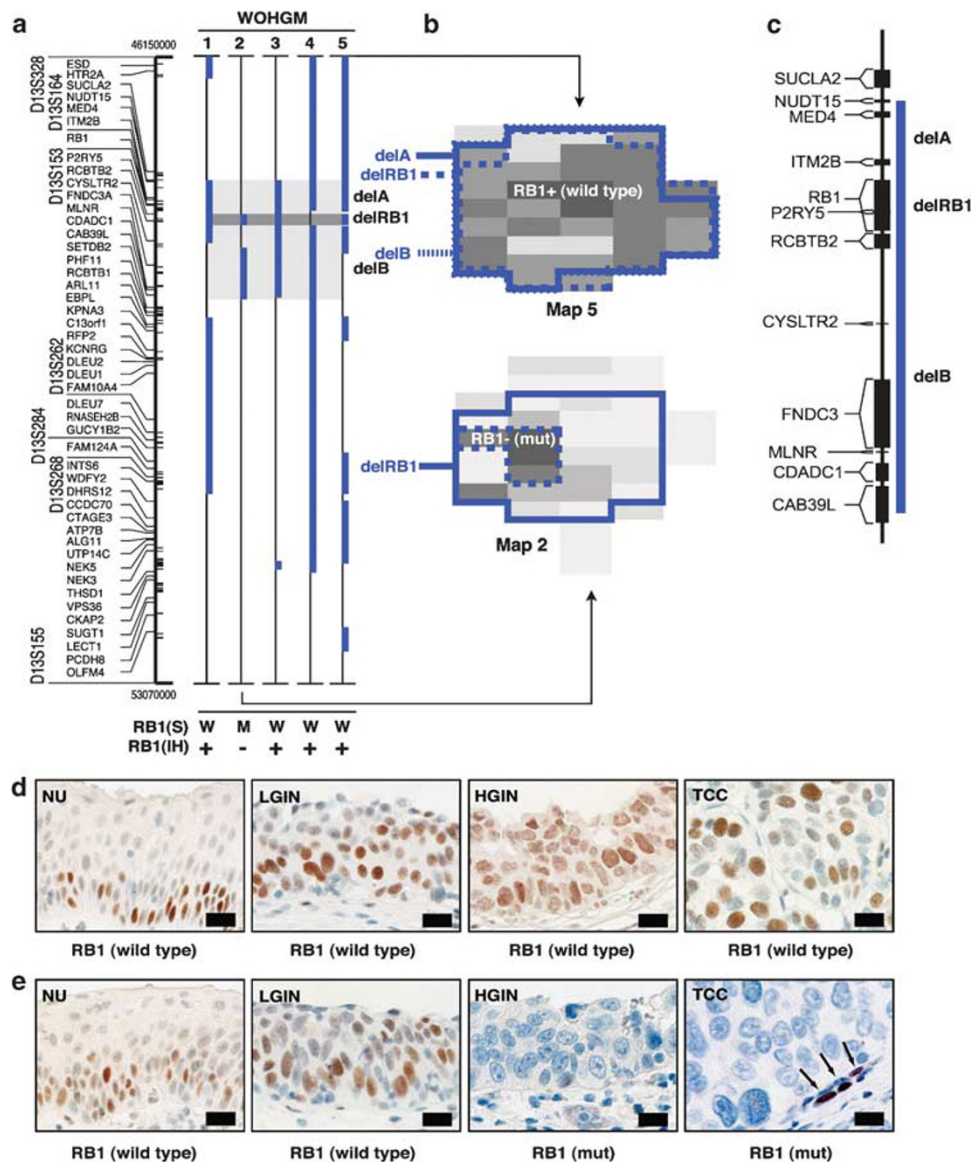
Figure 10 Integration of LOH and LOP patterns identified in the 13q14 region with *RB1* sequencing data and RB protein expression implicating the involvement of FR genes in the intraurothelial expansion of a neoplastic clone. (**a**) Regions of LOP associated with early clonal expansion identified by WOHGM with SNPs in five cystectomy specimens related to the status of *RB1* sequence, *RB1*(S), and RB protein expression revealed by immunohistochemistry, RB(IH), are illustrated. The results of *RB1* sequencing and immunohistochemical studies for RB protein expression are tabulated below the maps of individual bladders. W, wild-type *RB1*; M, mutant *RB1*. The mutation in map 2 involved codon 556 of exon 17 consisting of CGA→TGA and resulting in the change of Arg to a stop codon. The presence of immunohistochemically detectable RB protein is designated by +. The absence of RB protein expression is designated by −, and its distribution pattern is shown in the lower panel of (**b**). The genome sequence map in which the positions of hypervariable markers as well as known genes are designated by the bars on the left side of map. The regions of LOP in five cystectomies (maps 1–5) are depicted by the blue solid bars. The shadowed areas labeled delA and delB designate the regions of LOP flanking *RB1* involved in the incipient expansion of a neoplastic clone. The shaded area labeled del*RB1* designates the segment of LOP corresponding to the position of *RB1* on the sequence genome map. (**b**) The distribution of clonal LOP involving *RB1* and the same regions shown in (**a**) for map 5 (upper panel) is depicted. The lower panel shows the distribution of the segment with LOP in map 2 depicted in (**a**). The code for histologic map is shown in Figure 3. (**c**) Region of clonal LOP associated with growth advantage of *in situ* neoplasia identified by SNP-based mapping. (**d**) The immunohistochemical pattern of RB protein expression in representative mucosal samples of map 5 illustrated in (**b**) as the upper panel and corresponding to NU, LGIN, HGIN, and TCC is shown. The presence of RB protein in all mucosal samples correlated with the sequencing data, which indicated that the remaining wild-type *RB1* allele was retained in this case. (**e**) The immunohistochemical pattern of RB protein expression in representative mucosal samples of map 2 illustrated in the lower panel of (**b**). Positive nuclear staining for RB1 protein in stromal endothelial cells serves as an internal positive control (arrows). Note the absence of RB protein expression in HGIN and TCC corresponding to an area containing a mutant *RB1* allele. Solid black bars within photomicrographs indicate 50 μm. (Reprinted with permission from Lee S, Jeong J, Majewski T, *et al*. Proc Natl Acad Sci USA 2007;104:13732–13737.)
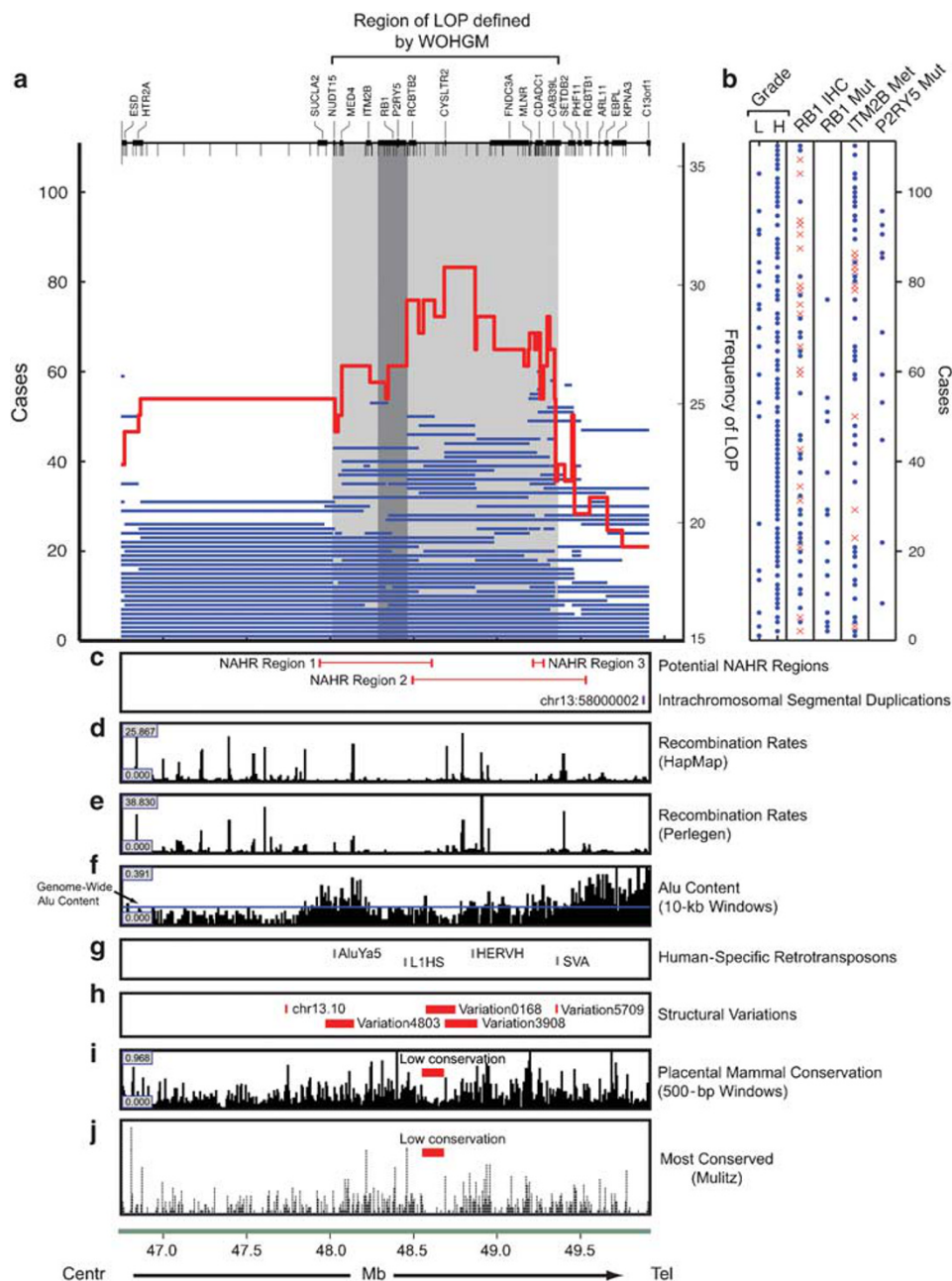
Figure 11 Map of LOP within 3.16-Mb segment around *RB1*. (**a**) Allelic losses were tested on 111 paired samples of bladder tumors and peripheral blood using SNP multiplex technology. Predicted sizes of LOP are depicted as blue bars and a continuous red line shows their frequency. The genomic map above the diagram shows positions of individual genes (solid black bars) and tested SNPs (thin black downward bars). Our previously published data were based on mapping of 84 paired samples of bladder tumor and peripheral blood DNA with 100 SNPs. The selected SNPs were located primarily inside and around the known and predicted genes within the tested region with a mapping gap centromeric to *RB1* between the genes *HTR2A* and *SUCLA2*. The absence of SNPs spanning a long segment centromeric to *RB1* might have resulted in an artificial shift of the deletion frequency curve telomeric to *RB1*. To address this concern, we tested additional eight SNPs spanning a gap between *HTR2A* and *SUCLA2* and increased the number of tested paired bladder tumor and non-tumor DNA samples to 111. The pattern and frequency of allelic loss generated by this approach were almost identical to our previously data[16] and implies that the most frequent breakpoint is located between *RCBTB2* and *CDADC1*. Overall, the pattern of allelic losses suggests the presence of additional candidate FR genes mapping telomerically to *RB1*. (**b**) The allelic losses are related to histologic grade, RB protein expression, *RB1* mutation, methylation of *ITM2B*, and nucleotide substitutions of *P2RY5*, as summarized in the diagram on the right. Details of *RB1* sequencing were published previously.[16] L, low grade (grade 1–2); H, high grade (grade 3); solid blue dots indicate the absence of RB protein expression, mutation of *RB1*, methylation of *ITM2B*, and nucleotide substitutions in *P2RY5*. Red crosses indicate tests not performed. (**c**) Putative NAHR regions identified by the presence of similar sequences in the same orientation using Human Chained Self Alignment browser. (**d**) Recombination rates based on HapMap. (**e**) Recombination rate based on Perlegen. (**f**) Alu repeat content per 10-kb windows. (**g**) Human-specific retrotransposons based on UCSC Alignment Nets. (**h**) Human polymorphic structural variants based on the Center for Applied Genomics Database of Genomic Variants and the UCSC Structural Var track. (**i**) Placental mammal conservation scores in 500-bp windows. (**j**) Most conserved elements, 28-way vertebrate Multiz alignment.
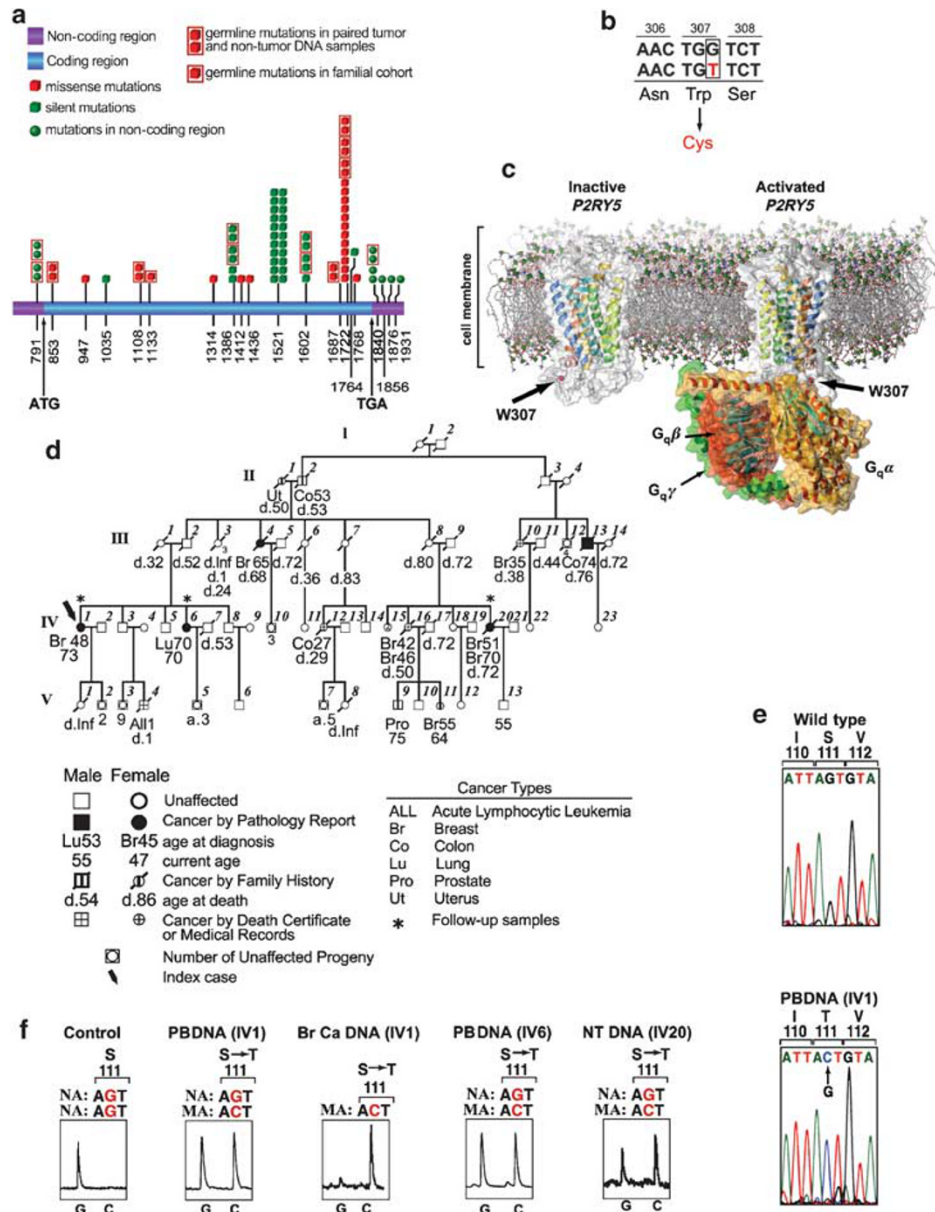
Figure 12 Nucleotide substitutions of *P2RY5* in sporadic and hereditary cancers. (**a**) Summary of sequence analysis of *P2RY5*. The positions of nucleotide substitutions are shown on the full-length mRNA. Details of sequencing are provided in Supplementary Table 2. (**b**) A G-T polymorphism at codon 307 in the PBDNA resulting in substitution of cysteine for tryptophan was identified by pyrosequencing (same case as shown in (**d**)). (**c**) A model of inactive *P2RY5* containing seven transmembrane (H1–H7) and one cytoplasmic (H8) helix structures showing the position of polymorphism in codon 307 located within the cytoplasmic domain of the protein (left diagram) that may affect its interaction with the $G_{\alpha\beta\gamma}$ trimeric protein complex (right diagram). (**d**) Pedigree of a family affected by several common human malignancies that include cancers of the breast, lung, colon, prostate, and uterus as well as acute leukemia. Sequencing of the peripheral blood DNA in individual IV1 identified a mutation of *P2RY5*. (**e**) Wild-type sequence of *P2RY5* (upper panel). A missense G-C mutation involving codon 111 and resulting in substitution of threonine for serine (S→T) documented by sequencing with subcloning of peripheral blood DNA from individual IV1 shown in (**d**) (lower panel). (**f**) Confirmation of a missense G-C mutation involving codon 111 of *P2RY5* in individuals IV1, IV6, and IV20 by pyrosequencing (same family as shown in (**d**)). Note a loss of wild-type *P2RY5* allele and retention of a mutant *P2RY5* in breast cancer cells from individual IV1. PBDNA, peripheral blood DNA; Br Ca DNA, DNA extracted from breast cancer cells microdissected with laser from paraffin-embedded tissue.

inactivation was a later event corresponding to onset of severe dysplasia/carcinoma *in situ* progressing to invasive carcinoma (Figure 10b and e).

The patterns of integrated LOH and LOP identified by microsatellite and SNP markers, respectively, from five

cystectomy specimens defined a minimal region of 1.34 Mb associated with clonal expansion of *in situ* neoplasia around *RB1*. Since this region was defined by WOHGM using five cystectomies, we further investigated the frequency of its involvement in 111 paired samples of bladder tumors and
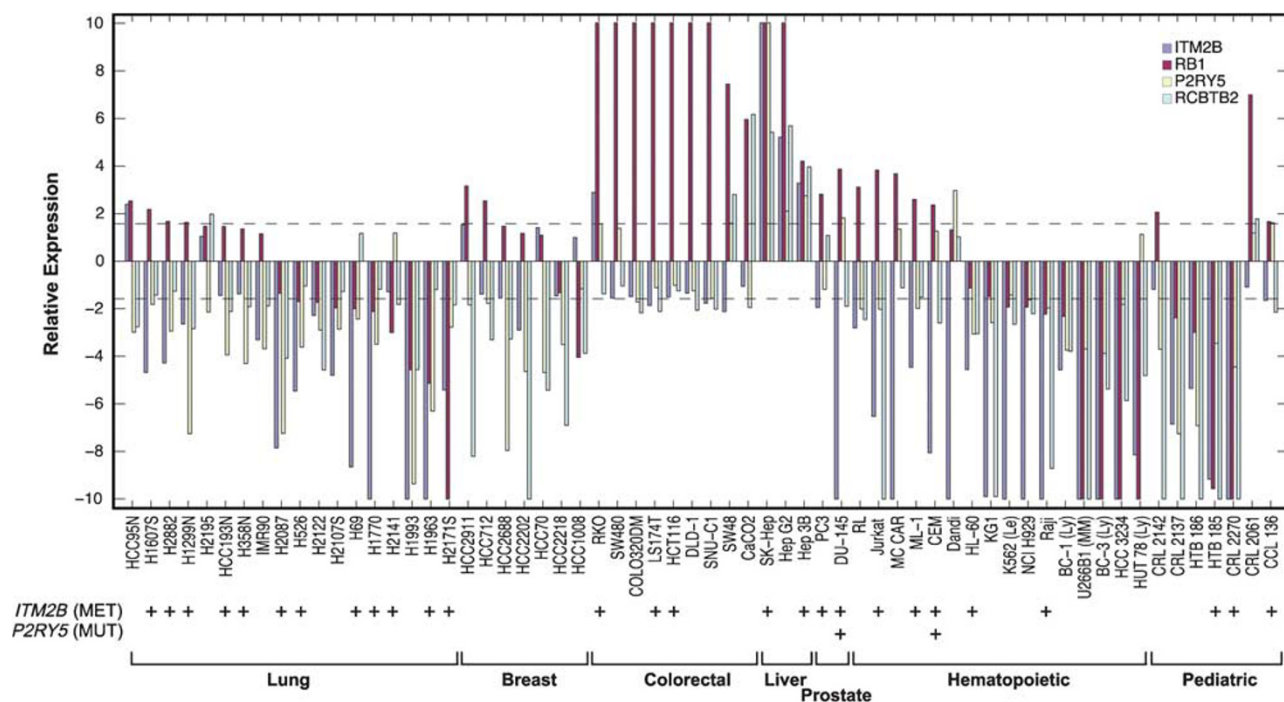
Figure 13 Inactivation of FR genes located within and around *RB1* is frequent in many cancer types. Results of quantitative RT-PCR analysis showing relative expression levels of FR genes and *RB1* in 62 cell lines derived from major groups of common human malignancies. The expression levels of each gene were compared to their baseline expression in the corresponding normal tissue. The presence of hypermethylation of the *ITM2B* promoter and mutations of *P2RY5* are summarized below the diagram. The relative expression levels of FR genes and *RB1* were calculated in comparison to the levels of their normal respective tissues. Note that cell lines derived from colorectal and liver cancers, which in general develop without involvement of *RB1* do not show downregulation of the FR genes. Dashed lines designate 90% confidence intervals. Details of sequence analysis of *P2RY5* are provided in Supplementary Table 1.

PBDNA by the allelotyping of 100 SNPs mapping to a 3.16-Mb segment around *RB1* (Figure 11a and b). The position of the segment with the most frequent LOP identified by this approach, overlapped with the position of the region associated with clonal expansion was initially found by WOHGM. LOP involving 3.16-Mb segment flanking *RB1* could be detected in 55% of the 111 TCC samples. In 28% of those cases, it contiguously involved *RB1* and its flanking regions. In an additional 19% of all tumor samples, it was restricted to regions flanking *RB1*. LOP involving this region was equally frequent in the two pathogenetic subsets of bladder cancers, and could be documented in 47% of low-grade (grade 1–2) superficial (T_a–T_{1a}) and 58% of high-grade (grade 3) invasive (T_{1b} and higher) TCCs ($P = 0.5$). In contrast, the inactivation of *RB1* as documented by the absence of RB protein expression in tumor cells by immunohistochemical analysis with the remaining mutant *RB1* allele revealed by DNA sequencing was predominantly seen in high-grade invasive TCC.

These data supported the hypothesis that genes or non-coding sequences located near the model tumor suppressor, *RB1*, may contribute to the development of bladder cancer by providing growth or survival advantage to the *in situ* neoplasia.

Genomic content of RB1 flanking region

To examine the genomic context of the minimal deleted region and its associated breakpoints, we performed a comprehensive analysis of the genomic content and sequence characteristics within the 3.16-Mb segment surrounding the *RB1* locus (Figure 11c–j).

Nonallelic homologous recombination (NAHR) is a major mechanism involved in rearrangements during mitotic crossover and DNA break repair causing somatic deletions frequently seen in sporadic human cancer.[77] NAHR between similar sequences in the same orientation leads to a reciprocal deletion and duplication between the chromosomes involved. A primary source of these similar sequences is mobile retrotransposon elements such as *Alu*s, which comprise about 11% of the human genome.[78] We analyzed the LOP region for putative sequences predisposing to NAHR by identifying similar sequences in the same orientation using Human Chained Self Alignments (University of California Santa Cruz (UCSC) Genome Browser) (Figure 11c). Two large partially overlapping regions bounded by similar sequences were identified. Potential NAHR region 1 (676 kb) is bounded by 474- and 429-bp segments that are primate specific, share 70% similarity and are comprised of ~38% long terminal repeat (LTR) retrotransposons. This region completely

Table 2 Summary of sequence, expression, and methylation analyses for 17 positional candidate FR genes and *RB1*

Gene name	Description	Sequencing		Expression	Methylation	
		Preliminary	Large scale	Downregulation	CpG island	Methylation
SUCLA2	Succinate-CoA ligase	ND	ND	−	+	−
NUDT15	Nudix-type motif 15	ND	ND	+	+	−
MED4	Mediator of RNA polymerase II transcription	ND	ND	−	+	−
ITM2B	Integral membrane protein 2B	−	−	+	+	+
RB1	Retinoblastoma 1, tumor suppressor	+	+	+	+	−
P2RY5	G-protein-coupled P2Y5 receptor	+	+	+	−	ND
RCBTB2	RCC1 and BTB domain-containing protein 2	−	ND	+	+	−
CYSLTR2	Cysteinyl leukotriene receptor 2	−	ND	−	−	ND
FNDC3A	Fibronectin type III domain-containing 3A	−	ND	−	+	−
MLNR	G-protein-coupled receptor 38	−	ND	+	+	+
CDADC1	Cytidine and dCMP deaminase domain	ND	ND	−	+	−
CAB39L	Calcium-binding protein 39-like	ND	ND	+	−	ND
SETDB2	SET domain, bifurcated 2	ND	ND	−	+	−
PHF11	PHD zinc-finger protein	ND	ND	−	+	−
RCBTB1	RCC1 and BTB domain-containing protein 1	ND	ND	+	+	−
ARL11	ADP-ribosylation factor-like tumor suppressor protein 1	ND	ND	+	−	ND
EBPL	Emopamil-binding protein-like	ND	ND	−	+	−
KPNA3	Karyopherin alpha 3 (importin alpha 4)	ND	ND	+	+	−

+, identification of mutations, downregulation, presence of CpG island, and methylation of the promoter, respectively. −, No evidence of mutation, downregulation, CpG island, and methylation of the promoter, respectively. ND, not done. Preliminary sequencing was performed on five cystectomy specimens used for WOHGM, 12 bladder cancer cell lines, and 20 bladder tumor samples comprising of 10 low-grade (grades 1 and 2) superficial (T_a–T_{1a}) and 10 high-grade (grade 3) invasive (T_{1b} and higher TCCs) showed no evidence of mutational inactivation. Large-scale sequencing of *P2RY5* was performed as described in Supplementary Table 2. The data on large-scale sequencing of *RB1* in bladder cancer were previously published.[16]
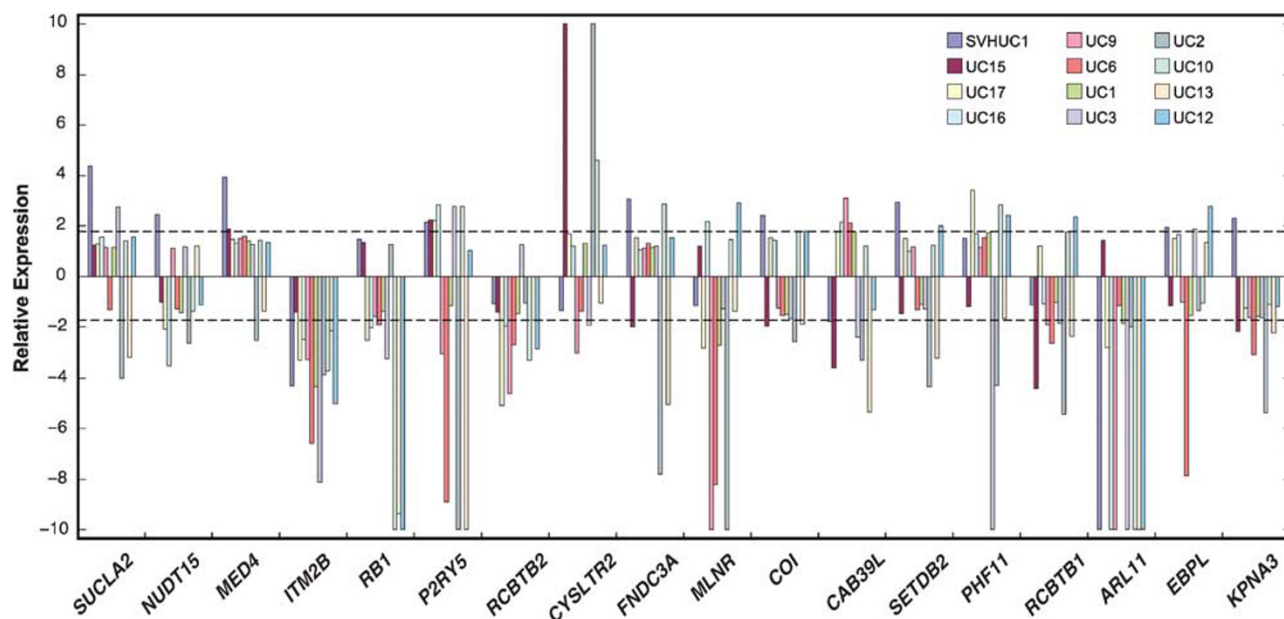
Figure 14 Expression pattern of candidate FR genes near *RB1*. Results of quantitative RT–PCR showing relative expression of 17 candidate FR genes and *RB1* in 12 bladder cancer cell lines compared to cultured normal urothelial cells (NU204).
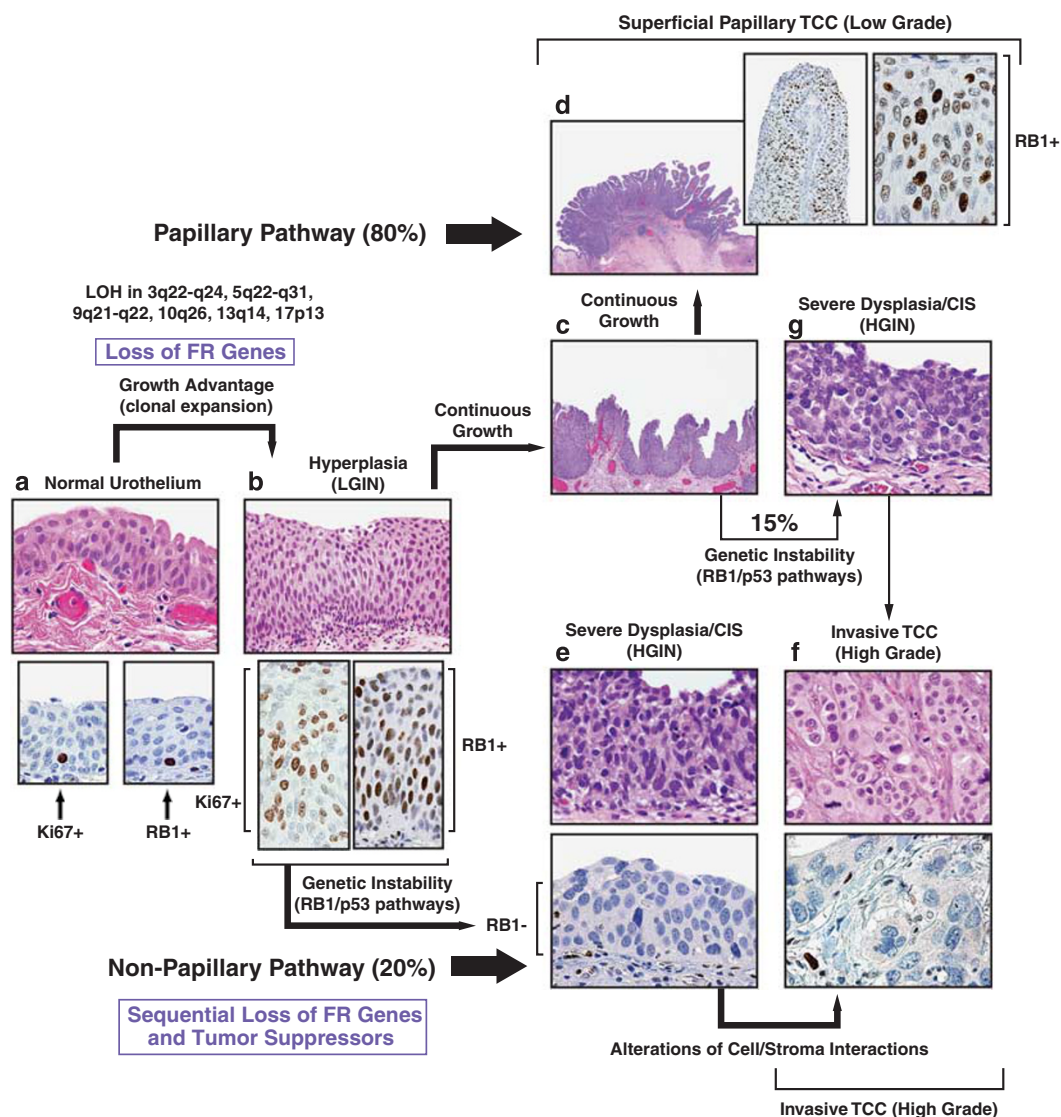
Figure 15 Dual-track concept of human bladder carcinogenesis. The expansion of preneoplastic clone, which shows minimal phenotypic deviation from the normal urothelium, is the incipient event in bladder carcinogenesis referred to as LGIN. In this phase, the loss of FR genes function provides growth advantage associated with the expansion of proliferating compartment. The proliferating cells expressing normal RB protein are seen in the entire thickness of LGIN. In contrast, normal urothelium contains only scattered proliferating cells expressing RB protein located in its basal layer. The continuous growth of LGIN leads to the development of low-grade superficial papillary TCC. In the non-papillary pathway, a successor clone with microscopic features of HGIN often shows a loss of major tumor suppressors such as *RB1* and has a high propensity for progression to an invasive high-grade non-papillary TCC. (**a**) Normal urothelium (upper panel). Expression of Ki67 in proliferating basal cells of normal urothelium (lower panel, left). Expression of RB protein in peribasal cells of normal urothelium (lower panel, right). (**b**) Urothelial hyperplasia with mild atypia referred to as LGIN (upper panel). Expression of Ki67 in the entire thickness of LGIN (lower panel, left); expression of RB protein in the entire thickness of LGIN (lower panel, right). (**c, d**) Low-grade superficial TCC with retention of expression of normal RB protein: insets to (**d**) show low- and high-power photomicrographs showing expression of normal RB protein in low-grade papillary TCC. (**e**) Severe intraurothelial dysplasia/carcinoma *in situ* (HGIN) (upper panel). Loss of RB protein expression in HGIN (lower panel). (**f**) High-grade invasive non-papillary carcinoma (upper panel). Loss of RB protein expression in high-grade invasive non-papillary TCC. Arrow shows expression of RB protein in endothelial cells adjacent to tumor, which serves as an internal positive control (lower panel). (**g**) Severe intraurothelial dysplasia/carcinoma *in situ* developing in bladder mucosa adjacent to a low-grade papillary tumor. It is responsible for switching the pathway and progression of some low-grade papillary tumors to high-grade invasive cancers.

encompasses six (*NUDT15*, *MED4*, *ITM2B*, *RB1 P2RY5*, and *RCBTB2*) genes and contains part of a seventh, *SUCLA2*. Potential NAHR region 2 (1053 kb) is bounded by the paralogous genes *RCBTB1* and *RCBTB2*. Comparative sequence analysis indicates that the *RCBTB* duplication event

is quite ancient, but the human *RCBTB* exonic sequences remain 72% similar. This region completely encompasses nine genes (*CYSLTR2*, *FNDC3A*, *MLNR*, *CDADC1*, *CAB39L*, *SETDB2*, *PHF11*, *RCBTB1*, and *RCBTB2*). Interestingly, deletion of *RCBTB1* has been suggested to be involved in the
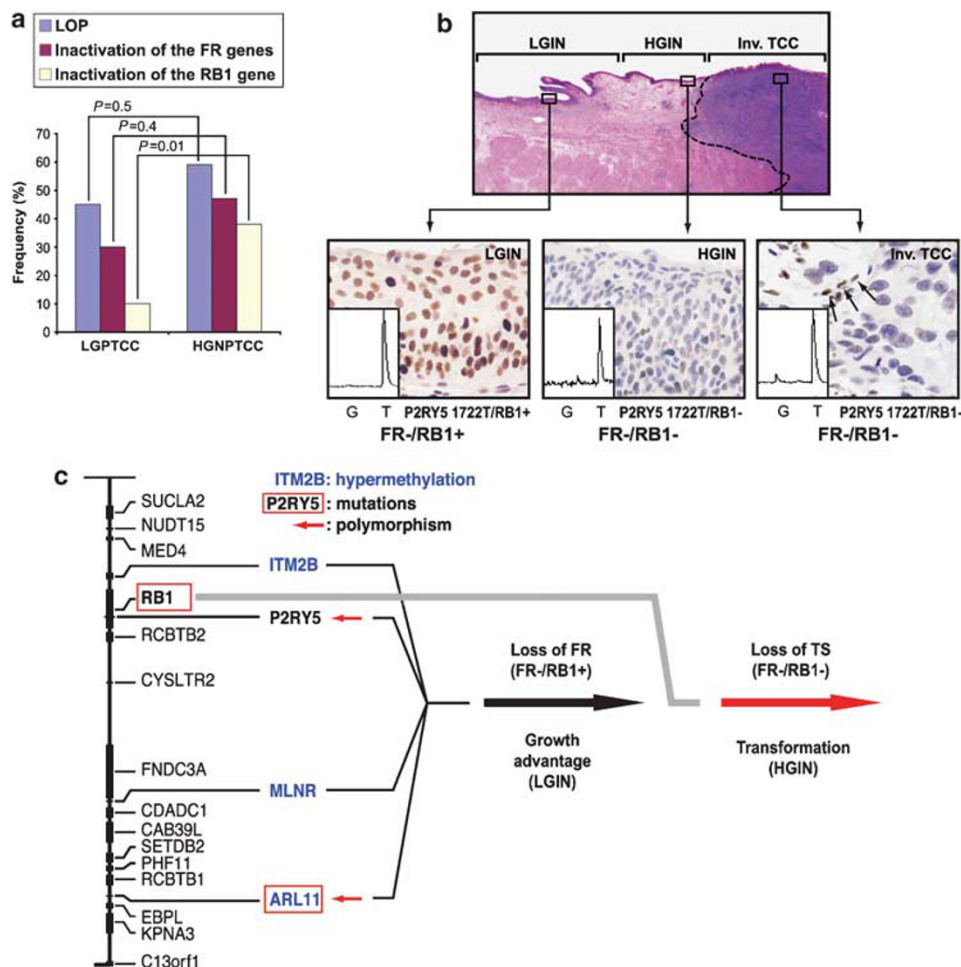
Figure 16 Inactivation of FR and *RB1* genes in the development of bladder cancer. (**a**) The analysis of LOP and inactivation of FR and *RB1* genes documented by DNA sequencing, methylation, and immunohistochemical analyses based on data shown in Figure 12. LGPTCC, low-grade (grades 1 and 2) superficial (T$_a$–T$_{1a}$) papillary TCC; HGNPTCC, high-grade (grade 3) non-papillary invasive (T$_{1b}$ and higher). (**b**) Sequential inactivation of *P2RY5* and *RB1* in the development of bladder cancer from *in situ* neoplasia. The loss of wild-type *P2RY5* copy and the retention of the 1722T variant allele inactivate the *P2RY5* gene. Low-power view of invasive bladder cancer and adjacent LGIN and HGIN (upper panel). Microdissected DNA corresponding to LGIN shows loss of wild-type *P2RY5* allele and retention of normal *RB* expression pattern (lower panel, left). Microdissected DNA corresponding to HGIN shows similar loss of wild-type *P2RY5* allele and additional loss of RB protein expression (lower panel, center). Similar loss of wild-type *P2RY5* allele and RB protein expression is seen in invasive TCC (lower panel, right). Arrows indicate retention of normal RB protein expression in endothelial cells adjacent to tumor. (Reprinted with permission from Lee S, Jeong J, Majewski T, *et al*. Proc Natl Acad Sci USA 2007;104:13732–13737.) (**c**) The FR gene hypothesis postulates that their inactivation by allelic loss, methylation, and less frequently by mutations or polymorphism contributes to the initial clonal expansion of *in situ* neoplasia microscopically consistent with LGIN common to both papillary and non-papillary pathways. The loss of tumor suppressor genes, such as *RB1*, is secondary and associated with the development of a successor clone showing features of severe dysplasia/carcinoma *in situ* (HGIN) progressing to invasive TCC.

development of B-cell chronic lymphocytic leukemia,[79,80] and *RCBTB2* is a candidate tumor suppressor for prostate cancer.[81] Potential NAHR region 3 (67 kb) is smaller than the other two regions and is bounded by 750- and 745-bp regions with 88% similarity. A total of 73% of the similarity regions are composed of *Alu* retrotransposons, and the gene *CDADC1* is completely contained within the region.

The three putative NAHR regions were compared to the deleted regions in our cancer samples. NAHR regions 1–3 were completely contained within 12, 5, and 26 cancer deletions, respectively. The positional relationship among the three NAHR regions and deleted segments could be identified

in 39% of bladder cancers, and involved the vast majority of TCCs demonstrating LOH/LOP in the 13q14 region.

Recombination hotspots that have a propensity toward allelic homologous recombination may also be involved in NAHR.[82] Therefore, we downloaded recombination rates based on HapMap and Perlegen[83] data from UCSC and found seven HapMap recombination hotspots within the LOP peak that have a recombination rate higher than the average chromosome 13 recombination rate of 1.28 cM/Mb (Figure 11d and e).[84]

Because *Alu*s are both fairly common and may cause genomic rearrangements implicated in human diseases,[85,86] we scanned the region for *Alu* content using 10-kb windows

(Figure 11f). We found the *Alu* density upstream of our LOP peak to be consistent with the 10.8% genome-wide average,[87] but the regions bordering this peak showed *Alu* densities as high as 39.1%.

Human-specific retrotransposons were identified by subtraction using all available mammalian Alignment Nets compared to human (UCSC Genome Browser) (Figure 11g). This method detected a human LINE-1 (L1HS) insertion in *RB1* that has previously been shown, in retinoblastoma patients, to result in deletion of *RB1* exon 24 through non-homologous recombination involving an MER repeat.[88] Human-specific *Alu* and SVA insertions were detected in the introns of *NUDT15* and *CAB39L*, respectively. A human endogenous retrovirus family H (HERVH) insertion in the LOP peak region was also detected and may play a role in cancer development.[89]

We scanned the region for known human polymorphic structural variants consisting primarily of duplications or deletions (Figure 11h). Several structural variants map to the interval, which provides further evidence of genomic instability across the region. These variants were identified in phenotypically normal individuals,[90] suggesting that a germline heterozygous loss of genomic sequence in the region may be associated with an increased risk for bladder cancer.

Finally, we computed average placental mammal conservation scores in 500-bp windows across the region along with placental mammal most conserved regions, derived from the 28 species conservation files downloaded from UCSC (Figure 11i and j).[91] These measurements show a region of low conservation within the LOP peak between the *RCBTB2* and *CYSLTR2* genes. Low conservation implies a lack of functional significance since functional regions are more conserved. It also implies that this region is highly diverse across species, suggesting instability over evolutionary time.

Taken together, these analyses suggest a number of potential mechanisms that may be involved in the generation of allelic losses affecting the *RB1* locus. Ongoing analyses are aimed at finding associations among unique genomic features of the region and risk for bladder cancer, as well as commonality between the features noted here and the remaining critical chromosomal regions identified by our WOHGM studies.

Alternative candidate FR genes mapping near RB1

The minimal region associated with clonal expansion of *in situ* neoplasia defined by a 1.34-Mb segment around *RB1* contains 11 positional candidate FR genes. Allelotyping of 100 SNPs mapping to a 3.16-Mb segment in 111 pairs of bladder tumor and PBDNA samples indicates that several additional genes mapping near the telomeric and centromeric borders of the region should also be considered positional candidate FR genes.

In our previous studies, we concentrated our efforts on the two neighbor candidate FR genes flanking *RB1*, namely

ITM2B and *RCBTB2* (*CHC1L*), as well as *P2RY5*, which is located inside *RB1*. We have shown that ectopically driven expression of a wild-type *ITM2B*, as well as *P2RY5*, reduced rates of proliferation in recipient cells and that these effects were associated with induction of apoptosis, as measured by proteolytic processing of procaspase-3 and DNA fragmentation. Because the 5′ regions of *ITM2B* and *RCBTB2* (*CHC1L*) contain CpG islands, we investigated whether methylation of the promoter region was responsible for silencing these genes in bladder cancer cell lines. Hypermethylation of the *ITM2B* promoter was identified in 50% of the cell lines, and was associated with significant reduction in gene expression. It was also detected in 40% of bladder tumor samples. We also documented that homozygous inactivation of *P2RY5* by allelic loss and mutation was antecedent to the loss of *RB1* in tumor development, and was associated with expansion of an *in situ* preneoplastic clone involving large areas of bladder mucosa.

Missense point mutations in *P2RY5* were found in 7% of TCC, and some of these mutations were germline alterations (Figure 12a). One of the polymorphic sites found in *P2RY5* (G1722 T) results in substitution of cysteine for tryptophan at position 307, and was detected in several bladder tumors and non-tumor DNA from the same patient. Molecular modeling of P2RY5 protein suggested that this substitution involving the cytoplasmic domain of the protein might affect its interaction with the G-protein complex, and compromise its biological activity (Figure 12b and c). We documented that the loss of a wild-type 1722 G *P2RY5* allele with retention of the variant 1722 T *P2RY5* allele occurred in the *in situ* phase of bladder neoplasia and preceded the loss of RB protein expression. We also found that all 1722 G-T carriers who were smokers developed bladder cancer, in a case–control study of 790 patients with bladder cancer.

Since our previously published data indicated that the germline nucleotide substitutions of *P2RY5* might represent a risk factor for hereditary cancer, we sequenced *P2RY5* in PBDNA from index cases of 46 families showing high predisposition for various common malignancies. We identified a germline mutation of *P2RY5* in one of these families (Figure 12d–f). Because several members of this family developed cancers of the breast, colon, lung, prostate, and uterus, we excluded the involvement of p53 and *BRCA1/2* by sequencing of PBDNA of the same index case, which confirmed wild-type sequences for all the genes. Given that the *P2RY5* gene is located within intron 17 of *RB1*, we excluded the coexistent mutation of *RB1* by complete sequencing of PBDNA of the same index case, which disclosed a wild-type sequence for *RB1*. By testing germline and breast tumor DNAs of additional members from this family, we showed that the tumors in the affected individuals had lost the wild-type allele and contained only a mutant *P2RY5*. The data were not sufficient for statistical analyses, but the transmission pattern in this family suggested a cosegregation of *P2RY5* germline mutations with the

malignant phenotype. Importantly, it was the whole-organ mapping of bladder cancer that led us to identify *P2RY5* germline mutations.

To further determine whether *ITM2B*, *P2RY5*, and *RCBTB2* (*CHC1L*) candidate FR genes were involved in other cancers besides TCCs, we analyzed their expression, methylation, and sequence in 62 cell lines derived from several major groups of common human malignancies. Of the cell lines tested, at least one of the FR genes was downregulated in 63% of the cases, and *ITM2B* was methylated in 42%, while mutations of *P2RY5* were detected in 5% (Figure 13). In addition, typically more than one candidate FR gene was downregulated in a given cell line. Interestingly, the cell lines derived from those tumors in which *RB1* had not been in general implicated in their development, such as colon and hepatocellular carcinomas,[92,93] retained high levels of FR gene expression.

Since our mapping data indicated that 17 genes within and near the minimal deleted region may represent positional candidate FR genes, we analyzed their expression, sequence, and methylation status (Table 2). In addition to previously studied *ITM2B*, *P2RY5*, and *RCBTB2* (*CHC1L*), the expression pattern of candidate FR genes indicates that *GPR38*, *CAB39L*, *RCBTB1*, and *ARL11* had more than a 50% reduction of their expression in several bladder cancer cell lines, and should be further investigated as putative FR genes (Figure 14). In addition to previously published data on *ITM2B*, *P2RY5*, and *RCBTB2* (*CHC1L*), a sequence analysis of new candidate FR genes *CYSLTR2*, *FNDC3A*, and *MLNR* (*GPR38*) in 12 bladder cancer cell lines and 20 bladder tumor samples comprising of 10 low-grade (grade 1–2) superficial (T_a–T_{1a}) and 10 high-grade (grade 3) invasive (T_{1b} and higher) TCCs showed no evidence of mutational inactivation.

To examine the candidate FR genes for potential epigenetic inactivation by DNA methylation, we first determined whether their predicted promoters were associated with CpG islands. Of the 17 genes studied, 14 have CpG islands in their promoter/exon 1 region, while 4 have CpG poor promoters (*P2RY5*, *CYSLTR2*, *CAB39L*, and *ARL11*). These latter four genes were not investigated further for DNA methylation. We determined the methylation status of the 14 CpG island-associated promoters, using COBRA in a panel of seven bladder cancer cell lines and SVHUCs. None of the genes were methylated in SVHUC cells. As previously described, *ITM2B* was significantly hypermethylated in several bladder cancer cell lines. Of the remaining 13 genes, 12 were unmethylated in all cell lines studied. One of the candidate FR genes, *MLNR* (*GPR38*), was highly hypermethylated in five out of seven cell lines and had a low level of methylation in the sixth. In summary, we identified two candidate FR genes (*ITM2B* and *MLNR*) whose CpG islands were significantly hypermethylated in multiple bladder cancer cell lines, in correlation with downregulation of their expression. Our data do not exclude the possibility of epigenetic inactivation

of the remaining positional candidate FR genes by other mechanisms such as chromatin modification. Chromatin modification may be particularly relevant for the candidate genes that show significant downregulation of their expression but do not contain CpG islands in their promoters.

The expression pattern of FR genes in multiple cell lines derived from several groups of human malignancies indicates that their downregulation is frequent in many cancer types. Hemizygous and homozygous deletions of 13q14 are frequent in a variety of hematopoietic and solid malignancies. Previously published data suggest the presence of several tumor suppressor-like candidate genes telomeric to *RB1*. *RCBTB1* and *RCBTB2* were implicated in the development of chronic lymphocytic leukemia and prostate cancer, respectively.[78,79] Several recent publications suggest that the inactivation of *ARL11* by hypermethylation, and less frequently by nucleotide substitutions including germline alterations, plays a role in the development of several common epithelial and hematopoietic malignancies.[94–98]

THE FR GENE CONCEPT AS RELATED TO BLADDER CARCINOGENESIS

Molecular events involved in the development of bladder cancer have been comprehensively discussed in several recent reviews.[4,5,99–102] In this section, we relate the pathogenesis of bladder cancer to our mapping data and the concept of FR genes.

It is generally accepted that human bladder cancer develops via two distinct, but sometimes overlapping pathways, papillary and non-papillary (Figure 15a–g). The so-called dual-track concept of bladder carcinogenesis was conceived in the 1970s, and was based on whole-organ histologic mapping data correlated with the clinical observations.[103–106] The distinct features of papillary and non-papillary types of bladder cancer were subsequently confirmed by several molecular studies showing that the tumor suppressors and oncogenes were primarily altered in the high-grade non-papillary pathway.[56,73,101,102,107–114] The early whole-organ mapping studies also suggested that both categories of bladder cancer emerge from the underlining *in situ* hyperplastic changes, referred to as LGIN. The similar frequency of losses in six chromosomal regions associated with the initial expansion of LGIN, seen in papillary and in non-papillary cancers, is in agreement with these observations and supports the concept that both pathways start as LGIN characterized by comparable patterns of chromosomal alterations. Whole-organ genetic mapping also indicates that the initial *in situ* expansion involves large areas of bladder mucosa forming clonal plaques, which clearly exceed the size of physiologic clonal areas seen in normal urothelium. Such normal clonal areas involve only 1.2 cm^2 and comprise approximately 2×10^6 cells.[115]

The genome-wide pattern of allelic loss implies a fluctuating rate of events with periods of instability, followed by relative stability associated with clonal expansion. The

sequence of events is clearly nonlinear and not identical in all tumors. It appears that a limited number of events have to occur to provide growth advantage for the initial clonal expansion. Among six chromosomal regions critical for the development of bladder cancer, high-resolution mapping data are available only for the 13q14 region containing the prototypic tumor suppressor, *RB1*. These data show that the loss of genetic material involving the minimally deleted region flanking the *RB1* gene, as well as inactivation of FR genes, is equally frequent in the superficial papillary and invasive high-grade non-papillary bladder cancers. Conversely, the inactivation of *RB1* is usually a later event, often seen in high-grade non-papillary invasive TCC (Figure 16a). These observations further support the common origin of both papillary and non-papillary tumors from the underlying LGIN.

Surprisingly and somewhat contradictory to these observations is the fact that the superficial papillary and high-grade invasive non-papillary tumors develop in the two distinct clinical settings; high-grade non-papillary tumors typically present *de novo* in patients with no history of superficial papillary tumors. The overlap, however, between the two pathways is reflected by the progression of superficial low-grade papillary lesions to high-grade invasive carcinomas. Such progression is preceded by the development of carcinoma *in situ* within a papillary lesion or in the adjacent areas of bladder mucosa, and occurs in approximately 15% of patients with a history of low-grade superficial papillary tumor. Consistent with the development of both pathways in the underlying LGIN and a distinct non-overlapping clinical presentation in most of the cases is the concept that continuous growth of the relatively stable LGIN leads to the development of superficial low-grade papillary TCC. In the high-grade non-papillary pathway, the initial LGIN is genetically unstable and results in the development of a successor clone or clones, with the inactivated tumor suppressor genes and microscopic features of HGIN progressing to an invasive high-grade TCC.

Collectively, our data provide evidence that supports the concept and existence of FR genes. Their loss of function in 13q14 promotes early clonal expansion of *in situ* neoplasia, microscopically defined as LGIN, and is antecedent to the loss of *RB1* function. In this phase, the loss of FR genes is responsible for the expansion of the proliferating compartment that expresses normal RB protein and occupies the entire thickness of *in situ* neoplasia (see Figure 15b). In contrast, normal urothelium contains only isolated peribasal cells that express RB protein. In this scenario, the FR genes provide the initial growth advantage for a neoplastic clone, whereas a subsequent loss of a tumor suppressor such as *RB1* is a transforming event associated with the development of HGIN progressing to invasive TCC (Figure 16b and c). According to this concept, the development of the high-grade aggressive form of bladder cancer is associated with the loss of FR genes followed by the loss of tumor suppressor genes

and activation of oncogenes. In this model, the continuous growth of genetically stable LGIN driven by the loss of genes with the FR-like function leads to the development of low-grade superficial papillary TCC.

CONCLUDING REMARKS

Our map depicts the evolution of genome-wide allelic losses in the development of a common human cancer, and provides a global look at genome involvement in carcinogenesis. It shows that each individual cancer developed through distinct patterns of genetic changes acting in concert with a succession of hits, providing growth advantage that resulted in clonal expansion and led to a gradual change of normal cells into cancer cells.[116,117] Although much work remains to be done to produce a complete, finished genome-wide map of bladder cancer development, we believe the significance of these data and their future applications include the following:

- The overall landscape of genomic alterations emerging from our data implicates a cumulative complex of allelic losses that occur in early phases of bladder neoplasia, even before precursor lesions such as dysplasia are microscopically detectable. However, only a small proportion of these losses demonstrate a close association with clonal expansion of *in situ* preneoplastic lesions and their progression to invasive cancer.
- Targeting of genes mapping to the chromosomal regions involved in clonal expansion of precursor lesions will help us to understand the early phases of human carcinogenesis, and may guide our future efforts to develop markers for early cancer detection and prevention.
- The analysis of human genome sequences spanning the involved chromosomal regions will not only reveal the gene content but may also provide unique clues to their structure and apparent instability based on the content of repeat elements, and other potentially unique evolutionary features. Such data can provide clues to structural genomic predispositions that lead to the involvement of distinct chromosomal regions.
- The map presented here should serve as a paradigm for the development of similar maps defining the development of other human cancers.
- The events of bladder cancer development identified by our studies may also be relevant to other cancers related to tobacco smoking and industrial or environmental exposure to chemical carcinogens, such as those that arise in the lung and upper aerodigestive tract.

The map presented here is but a snap shot of the currently available genome resources. The rapidly expanding databases of human genomic variation will necessitate a constant redrawing of the picture. High-resolution allelotyping with SNPs[118] should increase the resolution of our future maps and together with deeper population sequencing to define nucleotide, insertion/deletion, and copy number variation

will help point to which variants both individually and in combination are involved in the initiation and development of cancer.

1. Ayala AG, Ro JY, Amin M, (eds). Pathology of Incipient Neoplasia. Oxford University Press: New York, 2001.
2. Jemal A, Siegel R, Ward E, *et al.* Cancer statistics. CA Cancer J Clin 2007;57:43–66.
3. Lynch CF, Cohen MB. Urinary system. Cancer 1995;75(1 Suppl): 316–329.
4. Dinney CP, McConkey DJ, Millikan RE, *et al.* Focus on bladder cancer. Cancer Cell 2004;6:111–116.
5. Spiess PE, Czerniak B. Dual-track pathway of bladder carcinogenesis: practical implications. Arch Pathol Lab Med 2006;130:844–852.
6. Scher HI, Shipley WU, Herr HW, (eds). Cancer of the Bladder, 5th edn. Lippincott: Philadelphia, PA, 1997.
7. Vineis P, Pirastu R. Aromatic amines and cancer. Cancer Causes Control 1997;8:346–355.
8. Marcus PM, Vineis P, Rothman N. NAT2 slow acetylation and bladder cancer risk: a meta-analysis of 22 case–control studies conducted in the general population. Pharmacogenetics 2000;10: 115–122.
9. Chaturvedi V, Li L, Hodges S, *et al.* Superimposed histologic and genetic mapping of chromosome 17 alterations in human urinary bladder neoplasia. Oncogene 1997;14:2059–2070.
10. Czerniak B, Chaturvedi V, Li L, *et al.* Superimposed histologic and genetic mapping of chromosome 9 in progression of human urinary bladder neoplasia: implications for a genetic model of multistep urothelial carcinogenesis and early detection of urinary bladder cancer. Oncogene 1999;18:1185–1196.
11. Czerniak B, Li L, Chaturvedi V, *et al.* Genetic modeling of human urinary bladder carcinogenesis. Genes Chromosomes Cancer 2000;27:392–402.
12. Yoon DS, Li L, Zhang RD, *et al.* Genetic mapping and DNA sequence-based analysis of deleted regions on chromosome 16 involved in progression of bladder cancer from occult preneoplastic conditions to invasive disease. Oncogene 2001;20:5005–5014.
13. Kram A, Li L, Zhang RD, *et al.* Mapping and genome sequence analysis of chromosome 5 regions involved in bladder cancer progression. Lab Invest 2001;81:1039–1048.
14. Tuziak T, Jeong J, Majewski T, *et al.* High-resolution whole-organ mapping with SNPs and its significance to early events of carcinogenesis. Lab Invest 2005;85:689–701.
15. Kim MS, Jeong J, Majewski T, *et al.* Evidence for alternative candidate genes near *RB1* involved in clonal expansion of *in situ* urothelial neoplasia. Lab Invest 2006;86:175–190.
16. Lee S, Jeong J, Majewski T, *et al.* Forerunner genes contiguous to *RB1* contribute to the development of *in situ* neoplasia. Proc Natl Acad Sci USA 2007;104:13732–13737.
17. Mostofi FK, Sesternhenn IA, (eds). Histological Typing of Urinary Bladder Tumors. Springer: Berlin, New York, 1999.
18. Sobin LH, Wittekind Ch, (eds). International Union Against Cancer (UICC). TNM Classification of Malignant Tumors. John Wiley & Sons: New York, 1999.
19. Richter J, Jiang F, Gorog JP, *et al.* Marked genetic differences between stage pTa and stage pT1 papillary bladder cancer detected by comparative genomic hybridization. Cancer Res 1997;57:2860–2864.
20. Sen S, Zhou H, Zhang RD, *et al.* Amplification/overexpression of a mitotic kinase gene in human bladder cancer. J Natl Cancer Inst 2002;94:1320–1329.
21. Grossman HB, Wedemeyer G, Ren L, *et al.* Improved growth of human urothelial carcinoma cell cultures. J Urol 1986; 136:953–959.
22. Grossman HB, Wedemeyer G, Stein J. Autologous antibodies to human bladder cancer. Cancer Immunol Immunother 1988;26: 269–272.
23. Tanaka M, Koul D, Davies MA, *et al.* MMAC1/PTEN inhibits cell growth and induces chemosensitivity to doxorubicin in human bladder cancer cells. Oncogene 2000;19:5406–5412.
24. Liebert M, Wedemeyer G, Chang JH, *et al.* Comparison of antigen expression on normal urothelial cells in tissue section and tissue culture. J Urol 1990;144:1288–1292.
25. Christian BJ, Loretz LJ, Oberley TD, *et al.* Characterization of human uroepithelial cells immortalized *in vitro* by simian virus 40. Cancer Res 1987;47:6066–6073.
26. Phelps RM, Johnson BE, Ihde DC, *et al.* NCI-Navy Medical Oncology Branch cell line data base. J Cell Biochem 1996;24:32–91.
27. Gazdar AF, Minna JD. NCI series of cell lines: an historical perspective. J Cell Biochem 1996;24:1–11.
28. Lander ES, Linton LM, Birren B, *et al.* Initial sequencing and analysis of the human genome. Nature 2001;409:860–921.
29. Schuler GD. Electronic PCR: bridging the gap between genome mapping and genome sequencing. Trends Biotechnol 1998;16: 456–459.
30. Altschul SF, Gish W, Miller W, *et al.* Basic local alignment search tool. J Mol Biol 1990;215:403–410.
31. Ott J, (ed). Analysis of Human Genetic Linkage. John Hopkins University Press: Baltimore, 1995.
32. Hartigan J, (ed). Clustering Algorithms. John Wiley & Sons: New York, 1975.
33. Ronaghi M. Pyrosequencing for SNP genotyping. Methods Mol Biol 2003;212:189–195.
34. Ahmadian A, Gharizadeh B, Gustafsson AC, *et al.* Single-nucleotide polymorphism analysis by pyrosequencing. Anal Biochem 2000;280:103–110.
35. Xu HJ, Hu SX, Hashimoto T, *et al.* The retinoblastoma susceptibility gene product: a characteristic pattern in normal cells and abnormal expression in malignant cells. Oncogene 1989;4:807–812.
36. Xu HJ, Hu SX, Benedict WF. Lack of nuclear RB protein staining in G0/ middle G1 cells: correlation to changes in total RB protein level. Oncogene 1991;6:1139–1146.
37. Narod SA, Foulkes WD. BRCA1 and BRCA2: 1994 and beyond. Nature Rev 2004;4:665–676.
38. Ohayon T, Gershoni-Baruch R, Papa MZ, *et al.* The R72P P53 mutation is associated with familial breast cancer in Jewish women. Br J Cancer 2005;92:1144–1148.
39. Greenblatt MS, Chappuis PO, Bond JP, *et al.* TP53 mutations in breast cancer associated with BRCA1 or BRCA2 germ-line mutations: distinctive spectrum and structural distribution. Cancer Res 2001;61:4092–4097.
40. Figer A, Kaplan A, Frydman M, *et al.* Germline mutations in the PTEN gene in Israeli patients with Bannayan–Riley–Ruvalcaba syndrome and women with familial breast cancer. Clin Genet 2002;62: 298–302.
41. Tomlinson GE, Chen TT, Stastny VA, *et al.* Characterization of a breast cancer cell line derived from a germ-line BRCA1 mutation carrier. Cancer Res 1998;58:3237–3242.
42. Borg A, Isola J, Chen J, *et al.* Germline BRCA1 and HMLH1 mutations in a family with male and female breast carcinoma. Int J Cancer 2000;85:796–800.
43. Rubin SC, Blackwood MA, Bandera C, *et al.* BRCA1, BRCA2, and hereditary nonpolyposis colorectal cancer gene mutations in an unselected ovarian cancer population: relationship to family history and implications for genetic testing. Am J Obstet Gynecol 1998;178:670–677.
44. Moslehi R, Chu W, Karlan B, *et al.* BRCA1 and BRCA2 mutation analysis of 208 Ashkenazi Jewish women with ovarian cancer. Am J Hum Genet 2000;66:1259–1272.
45. Roa BB, Boyd AA, Volcik K, *et al.* Ashkenazi Jewish population frequencies for common mutations in BRCA1 and BRCA2. Nat Genet 1996;14:185–187.
46. Geisler JP, Hatterman-Zogg MA, Rathe JA, *et al.* Ovarian cancer BRCA1 mutation detection: protein truncation test (PTT) outperforms single

strand conformation polymorphism analysis (SSCP). Hum Mutat 2001;18:337–344.

47. Hogervorst FB, Cornelis RS, Bout M, *et al*. Rapid detection of BRCA1 mutations by the protein truncation test. Nat Genet 1995;10:208–212.

48. Clark SJ, Harrison J, Paul CL, *et al*. High sensitivity mapping of methylated cytosines. Nucleic Acids Res 1994;22:2990–2997.

49. Xiong Z, Laird PW. COBRA: a sensitive and quantitative DNA methylation assay. Nucleic Acids Res 1997;25:2532–2534.

50. Henson DE, Albores-Saavedra J, (eds). The Pathology of Incipient Neoplasia. Oxford University Press: New York, 2001.

51. Bishop JM. The molecular genetics of cancer. Science 1987;235: 305–311.

52. Fearon ER, Vogelstein B. A genetic model for colorectal tumorigenesis. Cell 1990;61:759–767.

53. Hanahan D, Weinberg RA. The hallmarks of cancer. Cell 2000; 100:57–70.

54. Ross RK, Jones PA, Yu MC. Bladder cancer epidemiology and pathogenesis. Semin Oncol 1996;23:536–545.

55. Sidransky D, Messing E. Molecular genetics and biochemical mechanisms in bladder cancer. Oncogenes, tumor suppressor genes, and growth factors. Urol Clin North Am 1992;19:629–639.

56. Simoneau AR, Jones PA. Bladder cancer: the molecular progression to invasive disease. World J Urol 1994;12:89–95.

57. Weinberg RA. Oncogenes, antioncogenes, and the molecular bases of multistep carcinogenesis. Cancer Res 1989;49:3713–3721.

58. Collins FS. Positional cloning: let's not call it reverse anymore. Nat Genet 1992;1:3–6.

59. Collins FS. Positional cloning moves from perditional to traditional. Nat Genet 1995;9:347–350.

60. Weinberg RA. Tumor suppressor genes. Science 1991;254:1138–1146.

61. Weinberg RA. The retinoblastoma protein and cell cycle control. Cell 1995;81:323–330.

62. Benedict WF, Murphree AL, Banerjee A, *et al*. Patient with 13 chromosome deletion: evidence that the retinoblastoma gene is a recessive cancer gene. Science 1983;219:973–975.

63. Sparkes RS, Murphree AL, Lingua RW, *et al*. Gene for hereditary retinoblastoma assigned to human chromosome 13 by linkage to esterase D. Science 1983;219:971–973.

64. Murphree AL, Benedict WF. Retinoblastoma: clues to human oncogenesis. Science 1984;223:1028–1033.

65. Friend SH, Bernards R, Rogelj S, *et al*. A human DNA segment with properties of the gene that predisposes to retinoblastoma and osteosarcoma. Nature 1986;323:643–646.

66. Lee WH, Bookstein R, Hong F, *et al*. Human retinoblastoma susceptibility gene: cloning, identification, and sequence. Science 1987;235:1394–1399.

67. Fung YK, Murphree AL, T'Ang A, *et al*. Structural evidence for the authenticity of the human retinoblastoma gene. Science 1987;236:1657–1661.

68. Friend SH, Horowitz JM, Gerber MR, *et al*. Deletions of a DNA sequence in retinoblastomas and mesenchymal tumors: organization of the sequence and its encoded protein. Proc Natl Acad Sci USA 1987;84:9059–9063.

69. Knudson Jr AG. Mutation and cancer: statistical study of retinoblastoma. Proc Natl Acad Sci USA 1971;68:820–823.

70. Horowitz JM, Park SH, Bogenmann E, *et al*. Frequent inactivation of the retinoblastoma anti-oncogene is restricted to a subset of human tumor cells. Proc Natl Acad Sci USA 1990;87:2775–2779.

71. Takahashi R, Hashimoto T, Xu HJ, *et al*. The retinoblastoma gene functions as a growth and tumor suppressor in human bladder carcinoma cells. Proc Natl Acad Sci USA 1991;88:5257–5261.

72. Ishikawa J, Xu HJ, Hu SX, *et al*. Inactivation of the retinoblastoma gene in human bladder and renal cell carcinomas. Cancer Res 1991;51:5736–5743.

73. Xu HJ, Cairns P, Hu SX, *et al*. Loss of RB protein expression in primary bladder cancer correlates with loss of heterozygosity at the RB locus and tumor progression. Int J Cancer 1993;53:781–784.

74. Bickers DR, Lowy DR. Carcinogenesis: a fifty-year historical perspective. J Invest Dermatol 1989;92(4 Suppl):121S–131S.

75. Doll R. An epidemiological perspective of the biology of cancer. Cancer Res 1978;38(11 Part 1):3573–3583.

76. Peto R, Roe FJ, Lee PN, *et al*. Cancer and ageing in mice and men. Br J Cancer 1975;32:411–426.

77. Weinberg RA, Hanahan D, (eds). The Molecular Pathogenesis of Cancer. Scientific American: New York, 1996.

78. Purandare SM, Patel PI. Recombination hot spots and human disease. Genome Res 1997;7:773–786.

79. Mabuchi H, Fujii H, Calin G, *et al*. Cloning and characterization of CLLD6, CLLD7, and CLLD8, novel candidate genes for leukemogenesis at chromosome 13q14, a region commonly deleted in B-cell chronic lymphocytic leukemia. Cancer Res 2001;61:2870–2877.

80. Solomou EE, Sfikakis PP, Kotsi P, *et al*. 13q deletion in chronic lymphocytic leukemia: characterization of E4.5, a novel chromosome condensation regulator-like guanine nucleotide exchange factor. Leuk Lymphoma 2003;44:1579–1585.

81. Latil A, Morant P, Fournier G, *et al*. CHC1-L, a candidate gene for prostate carcinogenesis at 13q14.2, is frequently affected by loss of heterozygosity and underexpressed in human prostate cancer. Int J Cancer 2002;99:689–696.

82. Lindsay SJ, Khajavi M, Lupski JR, *et al*. A chromosomal rearrangement hotspot can be identified from population genetic variation and is coincident with a hotspot for allelic recombination. Am J Hum Genet 2006;79:890–902.

83. Hinds DA, Stuve LL, Nilsen GB, *et al*. Whole-genome patterns of common DNA variation in three human populations. Science 2005;307:1072–1079.

84. Kong A, Gudbjartsson DF, Sainz J, *et al*. A high-resolution recombination map of the human genome. Nat Genet 2002; 31:241–247.

85. Deininger PL, Batzer MA. Alu repeats and human disease. Mol Genet Metab 1999;67:183–193.

86. Hedges DJ, Batzer MA. From the margins of the genome: mobile elements shape primate evolution. Bioessays 2005;27:785–794.

87. Grover D, Mukerji M, Bhatnagar P, *et al*. Alu repeat analysis in the complete human genome: trends and variations with respect to genomic composition. Bioinformatics 2004;20:813–817.

88. Albrecht P, Bode J, Buiting K, *et al*. Recurrent deletion of a region containing exon 24 of the *RB1* gene caused by non-homologous recombination between a LINE-1HS and MER21B element. J Med Genet 2004;41:e122.

89. Yi JM, Kim HM, Kim HS. Human endogenous retrovirus HERV-H family in human tissues and cancer cells: expression, identification, and phylogeny. Cancer Lett 2006;231:228–239.

90. Redon R, Ishikawa S, Fitch KR, *et al*. Global variation in copy number in the human genome. Nature 2006;444:444–454.

91. Siepel A, Bejerano G, Pedersen JS, *et al*. Evolutionarily conserved elements in vertebrate, insect, worm, and yeast genomes. Genome Res 2005;15:1034–1050.

92. Markowitz SD, Dawson DM, Willis J, *et al*. Focus on colon cancer. Cancer Cell 2002;1:233–236.

93. Bruix J, Boix L, Sala M, *et al*. Focus on hepatocellular carcinoma. Cancer Cell 2004;5:215–219.

94. Calin GA, Trapasso F, Shimizu M, *et al*. Familial cancer associated with a polymorphism in ARLTS1. N Engl J Med 2005;352: 1667–1676.

95. Sellick GS, Catovsky D, Houlston RS. Familial cancer associated with a polymorphism in ARLTS1. N Engl J Med 2006;354:1204–1205; author reply 1204–1205.

96. Masojc B, Mierzejewski M, Cybulski C, *et al*. Cancer familial aggregation (CFA) and G446A polymorphism in ARLTS1 gene. Breast Cancer Res Treat 2006;99:59–62.

97. Petrocca F, Iliopoulos D, Qin HR, *et al*. Alterations of the tumor suppressor gene ARLTS1 in ovarian cancer. Cancer Res 2006;66:10287–10291.

98. Castellvi-Bel S, Castells A, de Cid R, *et al*. Association of the ARLTS1 Cys148Arg variant with sporadic and familial colorectal cancer. Carcinogenesis 2007;28:1687–1691.

99. Knowles MA. Tumor suppressor loci in bladder cancer. Front Biosci 2007;12:2233–2251.

100. Knowles MA. Molecular subtypes of bladder cancer: Jekyll and Hyde or chalk and cheese? Carcinogenesis 2006;27:361–373.

101. Wolff EM, Liang G, Jones PA. Mechanisms of disease: genetic and epigenetic alterations that drive bladder cancer. Nat Clin Pract Urol 2005;2:502–510.

102. Wu XR. Urothelial tumorigenesis: a tale of divergent pathways. Nature Rev 2005;5:713–725.

103. Koss LG, Tiamson EM, Robbins MA. Mapping cancerous and precancerous bladder changes. A study of the urothelium in ten surgically removed bladders. JAMA 1974;227:281–286.

104. Koss LG, Nakanishi I, Freed SZ. Nonpapillary carcinoma *in situ* and atypical hyperplasia in cancerous bladders: further studies of surgically removed bladders by mapping. Urology 1977;9: 442–455.

105. Koss LG. Mapping of the urinary bladder: its impact on the concepts of bladder cancer. Hum Pathol 1979;10:533–548.

106. Koss LG. Bladder cancer from a perspective of 40 years. J Cell Biochem 1992;16I:23–29.

107. Fujimoto K, Yamada Y, Okajima E, *et al*. Frequent association of p53 gene mutation in invasive bladder cancer. Cancer Res 1992;52:1393–1398.

108. Cordon-Cardo C, Wartinger D, Petrylak D, *et al*. Altered expression of the retinoblastoma gene product: prognostic indicator in bladder cancer. J Natl Cancer Inst 1992;84:1251–1256.

109. Logothetis CJ, Xu HJ, Ro JY, *et al*. Altered expression of retinoblastoma protein and known prognostic variables in locally advanced bladder cancer. J Natl Cancer Inst 1992;84:1256–1261.

110. Spruck CH, Ohneseit PF, Gonzalez-Zulueta M, *et al*. Two molecular pathways to transitional cell carcinoma of the bladder. Cancer Res 1994;54:784–788.

111. Esrig D, Elmajian D, Groshen S, *et al*. Accumulation of nuclear p53 and tumor progression in bladder cancer. N Engl J Med 1994;331:1259–1264.

112. Cote RJ, Dunn MD, Chatterjee SJ, *et al*. Elevated and absent pRb expression is associated with bladder cancer progression and has cooperative effects with p53. Cancer Res 1998;58: 1090–1094.

113. Shariat SF, Tokunaga H, Zhou J, *et al*. p53, p21, pRB, and p16 expression predict clinical outcome in cystectomy with bladder cancer. J Clin Oncol 2004;22:1014–1024.

114. Chatterjee SJ, Datar R, Youssefzadeh D, *et al*. Combined effects of p53, p21, and pRb expression in the progression of bladder transitional cell carcinoma. J Clin Oncol 2004;22:1007–1013.

115. Tsai YC, Simoneau AR, Spruck CH, *et al*. Mosaicism in human epithelium: macroscopic monoclonal patches cover the urothelium. J Urol 1995;153:1697–1700.

116. Foulds L, (ed). Neoplastic Development. The Natural History of Cancer. Academic Press: New York, 1969.

117. Nowell PC. The clonal evolution of tumor cell populations. Science 1976;194:23–28.

118. Peiffer DA, Le JM, Steemers FJ, *et al*. High-resolution genomic profiling of chromosomal aberrations using Infinium whole-genome genotyping. Genome Res 2006;16:1136–1148.